the sub-continental lithospheric mantle?

David Orejana [a,*], Carlos Villaseca [a], Cecilia Pérez-Soba [a], José A. López-García [b], Kjell Billström [c]

[a] Department of Petrology and Geochemistry, UCM – CSIC, 28040, Madrid, Spain
[b] Department of Crystallography and Mineralogy, UCM, 28040, Spain
[c] Swedish Museum of Natural History, SE-104 05, Stockholm, Sweden

Keywords:
Gabbroic rocks
Crustal recycling
Variscan orogeny
Lithospheric mantle
Spanish Central System

A B S T R A C T

The gabbroic intrusions that crop out along the Spanish Central System (SCS) are geochemically heterogeneous, including primitive and evolved rocks. Differentiation is mainly related to fractionation of Cr-spinel and olivine, but mixing with coeval granitic magmas or crustal assimilation may have also played a role in the evolution of the most differentiated rocks. The most primitive uncontaminated gabbros show arc-like trace element chondrite and primitive-mantle normalised patterns, characterised by large ion lithophile elements (LILE)-light rare earth elements (LREE) enrichment, Sr and Pb positive and Nb–Ta–Ti negative anomalies. However, paleogeographic constraints suggest that the SCS was located far from subduction zones, so these geochemical signatures could be better explained by a recycling of continental crustal components within the mantle. The most primitive SCS gabbros expand the Sr–Nd isotopic compositional range of the Variscan basic magmatism in the Central Iberian Zone to more depleted values. This reflects a heterogeneous sub-continental lithospheric mantle under central Spain ranging from a depleted mantle ($\varepsilon Nd = +3.1$, $^{87}Sr/^{86}Sr = 0.704$) towards an isotopically enriched component ($\varepsilon Nd = -1.6$, $^{87}Sr/^{86}Sr = 0.706$). Geochemical modelling suggests that mantle enrichment could be explained by minor lower crustal metapelitic granulite contamination (~2%). Additionally, the Sr–Nd–Pb isotopic ratios of the most primitive gabbros match the composition of the European subcontinental lithospheric mantle recorded in ultramafic xenoliths from western and central Europe.

1. Introduction

The composition of the mantle can be studied using deep-seated ultramafic xenoliths entrained into alkaline volcanic rocks or by indirect means involving the geochemistry of mantle-derived primitive basic magmas. Many workers have dealt with the nature of the mantle under western and central Europe, by characterising the geochemistry of peridotite xenoliths transported by Cenozoic volcanic rocks (e.g., Wilson and Downes, 1991; Beccaluva et al., 2001; Downes, 2001; Witt-Eickschen et al., 2003; Beccaluva et al., 2004; Féménias et al., 2004; Berger et al., 2007). Mantle-derived xenoliths in Palaeozoic magmas are much more uncommon, having been described only in Scotland (Downes et al., 2001) and in the French Massif Central (Féménias et al., 2004).

In central Spain a suite of Upper Permian alkaline dykes carry pyroxenitic cumulates and granulites from the lower crust (Villaseca et al., 1999; Orejana et al., 2006), however peridotite mantle xenoliths have not been found. Nevertheless, successive intrusions of basic magmas (calc–alkaline, alkaline and tholeiitic) within the SCS from the end of the Variscan orogeny (Late Carboniferous) to the first stages of the rifting in Early Jurassic (Villaseca et al., 2004) provide valuable information regarding the underlying mantle. In this paper we study the SCS calc–alkaline gabbroic intrusions. Although they represent a small volume of magma in the SCS, other gabbroic calc–alkaline intrusions of similar age crop out in central Spain, either outside the SCS (Barbero et al., 1990; Barbero and Rogers, 1996; López-Moro and López-Plaza, 2004) or within the Central Iberian Zone (Dias and Leterrier, 1994; Galán et al., 1996; Bea et al., 1999; Bea, 2004). Much of the later work has highlighted the hybridization of the basic and acid Variscan magmas that gave rise to intermediate compositions, but also the enriched nature of the more primitive Variscan gabbros (e.g., Dias and Leterrier, 1994; Galán et al., 1996).

The isotopic enriched character of the Variscan SCS gabbros has been explained in terms of mantle enrichment due to the introduction of a crustal component beneath central Spain (Bea et al., 1999; Villaseca et al., 2004). Various mechanisms of lithospheric mantle enrichment in western and central Europe have been envisaged when studying several suites of metasomatised ultramafic xenoliths (Wilson and Downes, 1991; Becker et al., 1999; Beccaluva et al., 2001; Witt-

* Corresponding author. Department of Petrology and Geochemistry, Complutense University of Madrid, Calle José Antonio Novais 2, 28040, Madrid, Spain. Tel.: +34 91 394 5013; fax: +34 91 544 2535.
E-mail address: dorejana@geo.ucm.es (D. Orejana).

Eickschen et al., 2003; Féménias et al., 2004; Massonne, 2005; Berger et al., 2007). These include subduction-derived fluids, metasomatism by asthenospheric agents, or crustal components recycled into the mantle.

This paper presents a detailed petrographic and geochemical description of several SCS basic plutonic intrusions, including mineral, bulk and Sr–Nd–Pb isotope chemistry. Most of the samples show primitive chemical characteristics, with no significant traces of in-situ or syn-emplacement contamination.

2. Geological background

The SCS consists of a large granite batholith of ~10,000 km^2 (e.g., Bea et al., 1999; Villaseca and Herreros, 2000 and references therein) intruded within the Neoproterozoic to Palaeozoic metaigneous and metasedimentary series of the innermost continental region from the Variscan Iberian Belt (Fig. 1). The felsic batholith is made up by more than 100 intrusive units, most of them of monzogranitic composition, whose emplacement age ranges from 323 to 284 Ma (Villaseca et al., 1998 and references therein). These intrusions have been classified as 1) S-type peraluminous cordierite-bearing granitoids, 2) I-type metaluminous amphibole-bearing granitoids and 3) transitional biotite granitoids of intermediate peraluminous affinity (Villaseca and Herreros, 2000). Three models for the origin of the SCS granitic batholith have been suggested: a) hybridization between crustal melts and mantle-derived magmas (Pinarelli and Rottura, 1995; Moreno-Ventas et al., 1995); b) variable degrees of crustal assimilation by mantle derived magmas (Ugidos and Recio, 1993; Castro et al., 1999); and c) partial melting of essentially crustal sources, either from lower crustal derivation (Villaseca et al., 1998, 1999) or from mid-crustal levels (Bea et al., 1999, 2003). The close resemblance in whole-rock geochemistry (including Sr–Nd–Pb–O isotopic data) between SCS granites and the lower crustal felsic granulite xenoliths carried by the SCS Permian alkaline dykes, points to the lower crust as the most likely crustal source for the formation of the SCS batholith (Villaseca et al., 1999, 2007).

Five basic to intermediate magmatic suites (Gb1 to Gb5; Villaseca et al., 2004 and references therein) (Fig. 1) intruded this region during the Carboniferous to Early Jurassic. Gb1 comprises gabbroic to quartzdioritic intrusions that were mostly coeval with the granitoids. Geochronological data on these rocks (Rb–Sr isochron method) yielded ages ranging from 322 to 310 Ma (Casillas et al., 1991; Bea et al., 1999) whereas single-zircon dating indicated 312–305 Ma (Montero et al., 2004). Recent ion-microprobe U–Pb zircon studies constrain the range to more recent ages (306–305 Ma; Bea et al., 2006; Zeck et al., 2007).

The other mafic magmas from Gb2 to Gb5 are post-collisional dyke swarms. Gb2 and Gb3 are medium-K calc–alkaline to shoshonitic microgabbros respectively, with a poorly constrained age around 290 Ma (Rb–Sr whole-rock isochron; Galindo et al., 1994). The Gb4 alkaline suite, whose age ranges from 264 Ma (Ar–Ar in amphibole; Perini et al., 2004; Scarrow et al., 2006) to 252 Ma (U–Pb in zircon; Fernández Suárez et al., 2006), is represented by basic-ultrabasic lamprophyres and diabases together with monzo-syentic dykes. These rocks have been interpreted in terms of the introduction of a new mantle-derived magmatic component (isotopically similar to the PREMA compositional field), thus suggesting a significant geodynamic change in the SCS (Orejana et al., 2005, 2008). The last magmatic event recorded in the SCS is the large gabbroic Messejana-Plasencia tholeiitic dyke (Gb5), which has been dated at 203 Ma (Ar–Ar in biotite; Dunn et al., 1998). This latter magmatism has been related to the opening of the central Atlantic Ocean (e.g., Cebriá et al., 2003).

Moreno-Ventas et al. (1995) describe mixing processes with coeval granite magmas during emplacement for the Gb1 Variscan basic rocks from the Gredos Massif (Fig. 1). On the other hand, Bea et al. (1999) pointed to a hybrid mantle-lower crust source for the origin of these Gredos gabbros and Villaseca et al. (2004) suggested a role of crustal materials in the genesis of the Gb1 basic rocks via crustal recycling at mantle depths. In addition, several studies on other Iberian Variscan basic and intermediate intrusions suggest that crustal contamination at shallower levels is required to account for the geochemical variability of these rocks (Dias and Leterrier, 1994; Galán et al., 1996; López-Moro and López-Plaza, 2004; Vilá et al., 2005).

3. Analytical methods

The major element mineral compositions were determined at the *Centro de Microscopía Electrónica "Luis Bru" (Complutense University of Madrid)* using a JEOL JZA-8900 M electron microprobe with four wavelength dispersive spectrometers. Accelerating voltage was 15 kV and the electron beam current 20 nA, with a beam diameter of 5 μm. Counting time was 10 s on the peak and 5 s on each background position. The following mineral standards were used: sillimanite for Al; albite for Si and Na; almandine for Fe and Mn; kaersutite for Mg; microcline for K; ilmenite for Ti; Ni alloy for Ni and cromite for Cr. Corrections were made using the ZAF method. Analytical precision is 0.5–6% for oxides with concentration > 1.5 wt.% and < 10% for oxides with concentration < 1.5 wt.%.

The whole-rock composition of 24 gabbroic samples was determined at the Actlabs laboratories (Ontario, Canada) for major and trace elements. The fusion technique was used by employing lithium metaborate/tetraborate. The molten bead was then digested in a weak nitric acid solution. Samples have been analysed by inductively coupled plasma optic emission spectrometry (ICP-OES) for major elements, while trace elements have been determined by ICP mass spectrometry (ICP-MS), using a Thermo Jarrell Ash ENVIRO II simultaneous and sequential ICP or a Perkin Elmer Optima 3000 ICP. Uncertainties in major elements are always below 0.01%. All elements were analysed under the control of certified international standards (SY-3, NIST 694, W-2a, DNC-1, BIR-1 and GBW 07113). Further details on calibration, detection limits of trace elements, etc., can be found at http://www.actlabs.com/.

Sr–Nd isotopic data for 14 new gabbro samples were determined at the CAI de Geocronología y Geoquímica Isotópica of the Complutense University of Madrid, using an automated VG Sector 54 multicollector thermal ionisation mass spectrometer with data acquired in multi-dynamic mode. Isotopic ratios of Sr and Nd were measured on an aliquot of whole-rock powder. The Sr–Nd analytical procedures used in this laboratory have been described elsewhere (e.g., Reyes et al., 1997). Repeated analysis of NBS 987 gave $^{87}Sr/^{86}Sr = 0.710249 \pm 30$ (2σ, $n = 15$) and for the JM Nd standard the $^{143}Nd/^{144}Nd = 0.511809 \pm 20$ (2σ, $n = 13$). The 2σ error on calculated $\varepsilon(Nd)$ values is ± 0.4.

The Pb isotope ratios were determined on 7 gabbros at the Laboratory of Isotope Geology of the Natural History Museum of Stockholm. These samples were dissolved in a mixture of HF and HNO_3, and lead was separated by a full trace Pb chemical separation procedure, using specific ion-exchange columns. A ^{205}Pb tracer solution of known concentration was added to the samples to determine the lead contents. Isotope ratio analyses were done with a Finnigan MAT 261 TIMS run in multicollector mode. Over the course of this study, averaged values obtained for the Pb NBS 981 and NBS 982 were used to account for mass fractionation, following empirical relationships that vary as a function of temperature. The obtained data for unknowns, when corrected in an analogous way, are reproducible and accurate within 0.1% and analyses of the BCR-2 standard gave results in agreement with literature values.

4. Field relations, petrography and mineral chemistry

The gabbroic samples were collected from several small (usually < 2 km^2) plutonic bodies (Fig. 1). The intrusive bodies are hosted either by metamorphic rocks (e.g., Talavera, La Solanilla, Mercadillo,

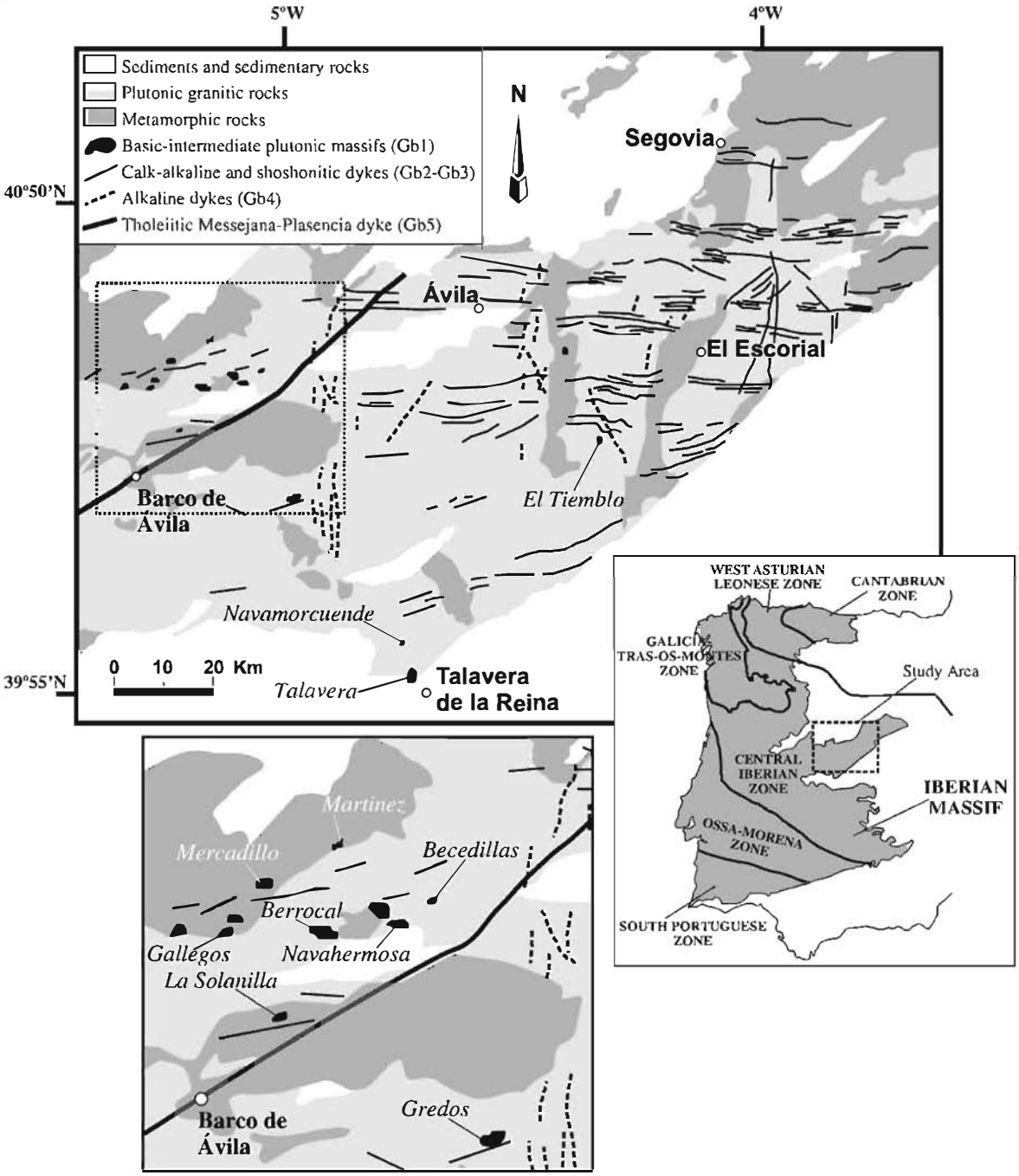

Fig. 1. Sketch geological map of the Spanish Central System showing the location of the gabbroic intrusions (and quartzdioritic massifs; e.g., El Tiemblo), as well as the post-Variscan basic and ultrabasic dyke swarms. Nomenclature Gb1 to Gb5 after Villaseca et al. (2004). The different zones defined for the Iberian Massif and an expanded view of a dense population of gabbroic plutons are shown separately.

Gallegos), or coeval granitic intrusions (e.g., Berrocal, Navahermosa, Becedillas). The latter also display outcrop-scale structures and textures indicative of mingling processes between the basic and acid magmas (see also: Casillas, 1989; Moreno-Ventas et al., 1995; Fernández et al., 1997). The most primitive rocks from these outcrops do not show evidence of magma mixing or crustal contamination (presence of different intermingled plutonic facies, enclaves, ocellar quartz, spongy plagioclase, and disequilibrium textures around minerals, etc.). However, felsic varieties (mainly quartzdiorites) with textures indicative of magma mixing were also sampled (e.g., Navahermosa massif).

Thus, the sampling ranged from olivine gabbro to amphibole-biotite-bearing quartzdiorite. Olivine-bearing gabbros are scarce and only present in four intrusions (Navahermosa, La Solanilla, Talavera and Mercadillo). The latter are medium- to coarse-grained norites to olivine gabbro-norites composed of anhedral, often rounded, relict crystals of olivine, euhedral to subhedral plagioclase, anhedral orthopyroxene and clinopyroxene, and interstitial (poikilitic) hydrous phases (phlogopite and pargasitic amphibole), usually accompanied by ilmenite.

Olivine, which never exceeds 13% in modal composition, may include Cr-spinel, and is often mantled by orthopyroxene. Some orthopyroxene show a symplectitic texture with neighbouring plagioclase. This, together with the generation of a secondary green-colourless amphibole (Mg-hornblende to actinolite and cummingtonite) at the expense of pargasite or clinopyroxene, can be interpreted

Table 1
Representative major element composition of the main minerals from the SCS gabbroic intrusions.

	Olivine				Orthopyroxene				Clinopyroxene				Mica			
Sample	108588	108585	107057	107042	108599	107038	107048	107053	108595	108601	108604	108585	107057	107048	108591	108604
	58	1	230	187	26	8	318	209	61	42	56	19	242	321	94	54
Location[a]	S	S	ME	T	NH	T	NM	B	G	NH	NH	S	ME	NM	S	NH
SiO_2	37.81	37.57	37.55	35.91	53.87	53.60	54.14	52.70	50.27	50.46	51.94	49.85	38.80	37.38	37.24	36.61
TiO_2	bdl	0.05	0.01	0.02	0.23	0.26	0.32	0.24	0.62	0.75	0.05	1.26	1.64	4.88	3.04	4.01
Al_2O_3	0.06	0.02	0.01	bdl	1.84	2.94	1.92	1.19	3.59	3.41	0.13	5.62	17.16	14.71	15.29	14.85
FeO[b]	23.47	25.61	29.24	36.94	9.91	12.56	15.98	22.02	4.54	6.62	11.16	7.65	8.78	12.56	15.78	19.00
Cr_2O_3	na	na	na	na	0.49	0.62	0.12	0.09	1.18	0.68	0.01	0.49	0.03	0.14	0.03	0.05
MnO	0.40	0.40	0.46	0.25	0.30	0.18	0.34	0.24	0.20	0.19	0.59	0.24	0.06	0.12	0.22	0.25
NiO	0.09	0.06	0.09	0.09	0.04	0.02	0.02	0.07	0.03	bdl	bdl	0.08	na	na	na	na
MgO	38.22	36.49	33.18	27.24	30.75	28.03	26.21	22.88	16.21	16.88	11.65	15.43	20.02	15.34	13.80	10.55
CaO	0.01	0.02	0.03	0.02	1.92	2.06	1.49	0.99	22.35	19.71	24.77	18.36	0.06	0.01	0.01	0.04
Na_2O	bdl	0.01	bdl	0.01	0.04	0.04	0.01	0.03	0.24	0.42	0.08	0.81	1.54	0.14	0.24	0.04
K_2O	bdl	bdl	bdl	0.01	0.01	0.01	bdl	bdl	bdl	0.01	bdl	0.01	7.46	9.47	9.91	9.76
Total	100.1	100.2	100.6	100.5	99.4	100.3	100.5	100.5	99.2	99.1	100.4	99.8	95.5	94.7	95.6	95.2
Mg#	0.74	0.72	0.67	0.57	0.85	0.80	0.75	0.65	0.86	0.82	0.65	0.78	0.80	0.69	0.61	0.50
Cations calculated on the basis of 4 O for olivine, 6 O for pyroxene and 24 (O, OH, F, Cl) for mica																
Si	0.990	0.992	1.004	1.000	1.904	1.906	1.949	1.947	1.854	1.862	1.959	1.834	5.290	5.230	5.830	5.860
Ti	0.000	0.001	0.000	0.000	0.006	0.007	0.009	0.007	0.017	0.021	0.002	0.035	0.170	0.510	0.360	0.480
Al	0.002	0.001	0.000	0.000	0.077	0.123	0.082	0.052	0.156	0.148	0.006	0.244	2.757	2.426	2.820	2.799
Fe	0.514	0.565	0.654	0.860	0.293	0.374	0.481	0.681	0.140	0.204	0.352	0.236	1.000	1.470	2.070	2.540
Cr	0.000	0.000	0.000	0.000	0.014	0.017	0.003	0.003	0.034	0.020	0.000	0.014	0.000	0.020	0.000	0.010
Mn	0.009	0.009	0.010	0.006	0.009	0.005	0.010	0.008	0.006	0.006	0.019	0.007	0.010	0.010	0.030	0.030
Ni	0.002	0.001	0.002	0.002	0.001	0.001	0.000	0.002	0.001	0.000	0.000	0.002	0.000	0.000	0.000	0.000
Mg	1.492	1.436	1.323	1.130	1.620	1.486	1.407	1.261	0.891	0.929	0.655	0.846	4.070	3.200	3.220	2.520
Ca	0.000	0.001	0.001	0.001	0.073	0.078	0.058	0.039	0.883	0.779	1.001	0.724	0.010	0.000	0.000	0.010
Na	0.000	0.000	0.000	0.001	0.003	0.003	0.001	0.002	0.017	0.030	0.005	0.058	0.410	0.040	0.070	0.010
K	0.000	0.000	0.000	0.000	0.000	0.000	0.000	0.000	0.000	0.001	0.000	0.000	1.300	1.690	1.980	1.990
Σcations	3.009	3.006	2.994	3.000	4.000	4.000	4.000	4.002	3.999	4.000	3.999	4.000	15.017	14.596	16.380	16.249

	Amphibole				Plagioclase				Cr-Spinel		
Sample	107042	107038	108595	108588	107042	107057	108601	108601	108585	108588	108585
	169	27	31	49	153	264	67 (core)	68 (rim)	11	42	4
Location[a]	T	T	G	S	T	ME	NH	NH	S	S	S
SiO_2	42.12	49.99	45.26	43.09	47.70	64.79	51.38	57.79	bdl	bdl	bdl
TiO_2	4.04	1.33	0.09	2.39	0.04	0.01	0.04	0.03	0.51	0.14	0.15
Al_2O_3	11.55	6.34	12.07	12.94	33.30	22.75	31.51	26.74	38.62	47.23	51.13
FeO[b]	12.97	8.21	9.46	10.45	0.12	0.22	0.08	0.13	29.15	25.30	24.98
Cr_2O_3	0.02	0.05	0.75	0.06	na	na	na	na	21.17	15.48	12.03
MnO	0.05	0.16	0.14	0.12	0.02	bdl	bdl	0.01	0.15	0.15	0.13
NiO	na	na	na	na	na	na	na	na	bdl	0.10	0.08
MgO	11.87	17.78	15.73	13.61	0.04	0.02	bdl	bdl	6.12	7.88	9.38
CaO	11.65	11.69	11.19	11.53	17.01	3.48	13.16	7.60	0.01	bdl	0.02
Na_2O	1.95	1.56	2.24	2.56	2.04	9.74	4.27	7.38	0.09	0.15	0.14
K_2O	1.07	0.42	0.20	0.43	0.02	0.04	0.06	0.15	bdl	bdl	0.01
Total	97.3	97.5	97.1	97.2	100.3	101.0	100.5	99.8	95.8	96.4	98.0
Mg#	0.62	0.79	0.75	0.70							
Cations calculated on the basis of 24 (O, OH, F) for amphibole and 32 O for plagioclase and Cr-Spinel											
Si	6.376	7.209	6.948	6.314	8.736	11.316	9.288	10.357	0.000	0.000	0.000
Ti	0.460	0.144	0.010	0.263	0.005	0.001	0.005	0.003	0.100	0.020	0.030
Al	2.058	1.077	2.182	2.233	7.183	4.678	6.708	5.644	11.380	13.150	13.750
Fe	1.642	0.990	1.215	1.280	0.019	0.032	0.012	0.019	6.100	5.000	4.770
Cr	0.003	0.006	0.091	0.007	0.000	0.000	0.000	0.000	4.180	2.890	2.170
Mn	0.006	0.019	0.018	0.015	0.003	0.000	0.000	0.001	0.030	0.030	0.030
Ni	0.000	0.000	0.000	0.000	0.000	0.000	0.000	0.000	0.000	0.020	0.020
Mg	2.679	3.823	3.600	2.973	0.010	0.005	0.000	0.000	2.280	2.780	3.190
Ca	1.890	1.805	1.840	1.810	3.337	0.650	2.549	1.459	0.000	0.000	0.000
Na	0.572	0.436	0.667	0.727	0.724	3.299	1.497	2.565	0.040	0.070	0.060
K	0.207	0.077	0.038	0.080	0.004	0.009	0.014	0.033	0.000	0.000	0.000
Σcations	15.893	15.586	16.609	15.702	20.021	19.990	20.083	20.091	20.091	20.091	20.091

[a] B: Becedillas; G: Gallegos; ME: Mercadillo; NH: Navahermosa; NM: Navamorcuende; S: La Solanilla; T: Talavera.
[b] Fe total expressed as FeO. na: not analised; bdl: below detection limit.

in terms of subsolidus re-equilibration. These rocks usually have hypidiomorphic intergranular subophitic textures. Clear cumulus textures are lacking. Olivine and plagioclase are the earlier minerals to precipitate (occasionally accompanied by clinopyroxene and orthopyroxene), while phlogopite and amphibole are always interstitial phases. The above textures suggest the following order of crystallization: Cr–Spinel + Olivine + Plagioclase + Orthopyroxene + Clinopyroxene → Phlogopite + Amphibole + Ilmenite. Common accessory minerals are apatite, titanite, monazite, baddeleyite and zircon.

Quartzdiorites have been found in several gabbroic outcrops and are mainly composed of plagioclase, biotite and interstitial quartz, while some samples also have Fe-rich clinopyroxene. These rocks have equigranular to inequigranular texture, with large plagioclase crystals with biotite and clinopyroxene inclusions. Some of the samples have

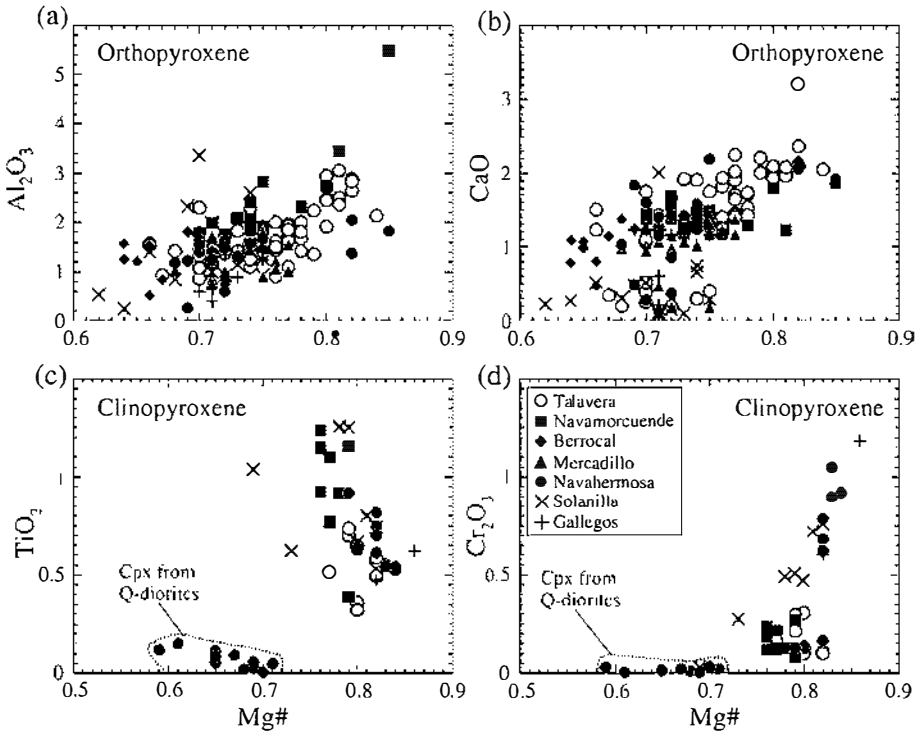

Fig. 2. Major element mineral chemistry (wt.%) of (a, b) orthopyroxene and (c, d) clinopyroxene from the SCS gabbroic intrusions.

subophitic and intergranular texture, characterised by plagioclase laths surrounded by poikilitic quartz, and intergranular biotite respectively. Ocellar xenocrystic quartz and zoned plagioclase with sericitized (originally Ca-rich) cores rimmed by andesine are also present in some of the samples. Amphibole in these relatively felsic rocks is usually secondary actinolite, which is abundant in strongly altered quartzdiorites.

Table 1 shows major element contents representative of the main constituent phases of the SCS gabbros. The primary mafic minerals do not show significant core to rim chemical zoning (e.g., Fo_{66} to Fo_{65} and En_{71} to En_{70}). Olivine, orthopyroxene and clinopyroxene from the most primitive samples have moderate to high Mg# numbers: Fo_{57} to Fo_{78}, En_{62} to En_{85} and 0.69 to 0.86 respectively. Olivine shows NiO and MnO contents below 0.15 wt.% and 0.5 wt.% respectively. Cr-spinel is usually included within olivine crystals and contains Al_2O_3 in the range 38.6–51.1 wt.% and Cr_2O_3 from 12 to 21.2 wt.%. Orthopyroxene has a marked heterogeneity, with Al_2O_3, CaO, TiO_2 and Cr_2O_3 contents reaching values of up to 5.5 wt.%, 3.2 wt.%, 0.67 wt.% and 0.66 wt.%, respectively (Fig. 2a, b). The clinopyroxene phase includes augite and diopside, being the latter present only in quartzgabbros and quartzdiorites. The Mg# value is positively correlated with Cr_2O_3 content (up to 1.2 wt.%) (Fig. 2d). TiO_2 and Al_2O_3 may reach 1.25 wt.% and 5.6 wt.% respectively, whilst CaO ranges from 11.5 to 22.5 wt.%. Clinopyroxene from the quartzdiorites is markedly different in composition, with lower Mg# (0.59–0.72), Al_2O_3 (<1.6 wt.%), TiO_2 (<0.15 wt.%) and Cr_2O_3 (<0.04 wt.%) and higher CaO (up to 25.5 wt.%) (Fig. 2c, d).

Plagioclase in both gabbros and quartzdiorites shows a heterogeneous composition ranging from bytownite (An_{74}) to oligoclase (An_{16}) (Fig. 3a). Contrary to the mafic phases, plagioclase crystals develop a clear core to rim normal zoning towards higher Na (Fig. 3a).

Brown primary calcic amphibole can be classified as pargasite, though according to the classification of Leake et al. (1997) it may also plot within the kaersutite and edenite compositional fields. In the primitive uncontaminated gabbros, amphibole Mg# varies from 0.61 to 0.78 (Fig. 3b) and the Cr_2O_3 composition reaches 0.75 wt.%. The amphibole is also characterised by high contents of TiO_2 (up to 5 wt.%) and Al_2O_3 (8–18 wt.%), and higher Na_2O (1.2–3.1 wt.%) compared to K_2O (0.2–1.2 wt.%). The abundant secondary amphibole can be classified as Mg-hornblende to actinolite, but also plots within the Mg-cummingtonite to cummingtonite series. Mica is a dominantly brown Ti-phlogopite in the primitive gabbros, with high TiO_2 (up to 4.9 wt.%) and Mg# numbers ranging from 0.65 to 0.86 (similar to those of clinopyroxene and orthopyroxene) (Fig. 3c). On the other hand, green Fe-rich biotite dominates within quartzdiorites, with Mg# from 0.43 to 0.64.

5. Whole-rock geochemistry

5.1. Major and trace elements

The samples selected for whole-rock geochemistry represent 10 basic-intermediate intrusions, ranging in modal composition from olivine gabbros to quartzdiorites. Their SiO_2 content and Mg# numbers range from 46 to 58 wt.% and from 0.50 to 0.75 respectively (Table 2). However, the most primitive samples have high Mg# with a limited range of 0.66 to 0.73.

All these rocks plot in the sub-alkaline field (except quartzdiorite 108591) of the Total Alkali–Silica (TAS) diagram (Fig. 4a), and are enriched in Na_2O relative to K_2O, with the only exception of one amphibole-rich rock (sample 107632). Besides, according to their SiO_2 and K_2O contents these rocks can be classified as medium-K (the most primitive samples) to high-K calc–alkaline rocks (Fig. 4b). The Berrocal and Becedillas outcrops plot in the high-K field. Previous studies on the SCS basic intrusions classified these rocks within the appinite suite (Bea, 2004), however their low alkalis content and petrographic characteristics (e.g., low modal amount and late interstitial character of primary amphibole in the SCS olivine gabbros) argue against this conclusion (see appinite compositional field in Fig. 4). Binary plots show an overall positive correlation of Mn, Cr and Ni with respect to Mg#, whereas this differentiation index is negatively correlated to the abundances of many major and trace elements (e.g., Si, Ti, Na, K, Rb,

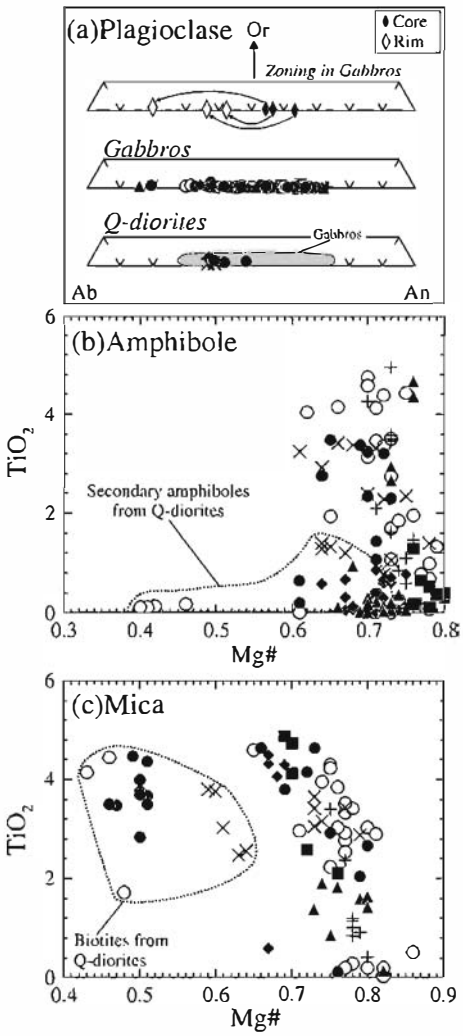

Fig. 3. Major element mineral chemistry (wt.%) of (a) plagioclase, (b) amphibole and (c) mica from the SCS gabbroic intrusions. Three core to rim zoning patterns in plagioclases have been illustrated separately in the plagioclase diagram. See other symbols in the legend from Fig. 2.

Ba, Zr, Nb, REE) (Fig. 5). This general trend is also observed at the single gabbroic intrusion scale (e.g., Berrocal). Most of the analyses have LOI values in a moderate range of 0.5–1.6 wt.% (Table 2). The Berrocal intrusion can be distinguished from the rest of the Mg-rich SCS gabbros due to its slightly higher LILE (K, Rb, Ba, Sr), Th–U and Nb–Ta contents, and lower Ca, Sc and V concentrations (Figs. 4 and 5). Similar to other Variscan gabbroic rocks from Western Europe, the SCS gabbros have remarkable lower Ba–Sr contents with respect to arc-related gabbros (e.g., Cesare et al., 2002; Claeson and Meurer, 2004).

The most Mg-rich gabbroic rocks have chondrite- and primitive mantle-normalised trace element abundances with LREE fractionated patterns and a nearly flat HREE slope ($Dy_N/Yb_N = 1.06–1.57$) (Fig. 6a). Concentrations of the most incompatible trace elements (Rb, Ba, Th, U and LREE) are high when considering quartzdiorite samples with moderate to low Mg# (Figs. 5 and 6b, d). Furthermore, negative Nb–Ta, P and Ti anomalies and peaks at Pb and Zr–Hf appear in all samples (Fig. 6c, d). Only four primitive gabbros from La Solanilla and Navahermosa plutons, and two quartzdiorite samples, show positive Eu and Sr anomalies. These samples have slightly higher Al_2O_3 and CaO contents (Fig. 5), which might be an indication of some degree of plagioclase accumulation. Nevertheless, the rest of the SCS gabbros show negative Sr and Eu anomalies.

5.2. Sr–Nd–Pb isotopes

Tables 3 and 4 show the results from 14 analyses for Sr and Nd isotopic ratios and 7 of common Pb from the SCS gabbroic intrusions. The isotope data were corrected for in-situ radiogenic growth assuming an average age of 305 Ma on the basis of the U–Pb zircon ages obtained by Bea et al. (2006) and Zeck et al. (2007).

The initial $^{87}Sr/^{86}Sr$ and εNd of the samples range from 0.7041 to 0.7068 and +3.1 to −4.4 respectively (Fig. 7). These radiogenic values correlate well and follow the differentiation trend of the mantle array, ranging from slightly depleted to slightly enriched. The variation of Sr–Nd isotopes in the whole dataset is also recorded within a single intrusion (e.g., samples from La Solanilla and Navahermosa massifs) (Fig. 7). If the most primitive samples are considered (Table 3), two groups of SCS gabbros can be separated on the basis of their initial Sr–Nd isotope ratios: a depleted group with positive εNd (Navahermosa, La Solanilla, Berrocal and Mercadillo) and an enriched group with higher $^{87}Sr/^{86}Sr$ (Talavera and Gallegos). Gabbros from the previously studied Gredos massif (Moreno-Ventas et al., 1995; Bea et al., 1999) overlap the compositional field of this second enriched group (Fig. 7). In this respect, the La Solanilla and Navahermosa gabbros show the most depleted Sr–Nd isotopic composition recorded in Variscan gabbroic rocks from the Central Iberian Zone (Fig. 7). This is indicative of the involvement of a more depleted mantle source than previously thought in the genesis of these basic rocks within the Variscan Iberian Belt. The SCS gabbroic intrusions also overlap the compositional field of the subsequent Permian calc–alkaline to alkaline dykes.

The Pb radiogenic values of the SCS gabbros cluster together in a reduced field (Fig. 8), showing $^{206}Pb/^{204}Pb$, $^{207}Pb/^{204}Pb$ and $^{208}Pb/^{204}Pb$ in the range 18.25–18.55, 15.61–15.64 and 38.21–38.84 respectively. These are the first Pb data available on SCS Iberian gabbros. Nonetheless, data from other basic intrusive rocks and deep-seated mafic and ultramafic xenoliths from the Spanish Central System have recently been published (Villaseca et al., 2007; Orejana et al., 2008), and they all have a composition close to that of these gabbroic bodies. Additionally, the $^{206}Pb/^{204}Pb$ ratios are similar to Prevalent Mantle (PREMA) or Bulk silicate Earth (BSE) components, whereas $^{207}Pb/^{204}Pb$ and $^{208}Pb/^{204}Pb$ tend to be higher.

6. Petrogenesis

6.1. Differentiation processes: crystal fractionation vs. magma mixing and assimilation

The SCS late Variscan gabbroic rocks are geochemically heterogeneous. With the sole exception of sample 107632 (altered amphibole-rich gabbro), the rest of gabbros have primitive compositions with Mg# values up to 0.73 and Cr and Ni concentrations up to 712 and 391 ppm, respectively (Table 2). The moderate Mg, Cr and Ni concentrations, together with the low contents of modal olivine and the absence of cumulate textures in the Mg-rich samples, indicate a non-cumulate origin. The heterogeneous modal composition of these rocks (olivine + plagioclase + orthopyroxene + clinopyroxene + amphibole + phlogopite + ilmenite), with early crystals in equilibrium with late interstitial phases, may represent crystallization from a single liquid. This conclusion is also in agreement with the mineral composition of these rocks: the An content in plagioclase is lower ($<An_{74}$) than those of typical arc-type cumulates ($>An_{82}$; Beard, 1986). Moreover, only four Mg-rich samples show a small positive Eu anomaly.

According to Frey et al. (1978) criteria for primary mantle melts (Mg# = 0.60–0.70; Cr = 500–1000 ppm and Ni = 200–500 ppm), the composition of the most primitive rocks would approximate that of their parental mantle magmas. Nevertheless, olivine from primary melts is usually confined to the range Fo_{88}–Fo_{94}, whereas olivine from the studied gabbros does not exceed Fo_{78}. Thus, it seems likely that

Table 2
Bulk chemistry of the SCS gabbroic intrusions.

Sample	107033	107039	107042	107038	107040	107048	107051	107053	107049	107050	107057	107055	107627	107632	107631	108591	108588	108585	108595	108596	108600	108599	108601	108604
Location[a]	TI	TA	TA	TA	TA	NM	BE	BE	BE	BE	ME	ME	MA	B	B	S	S	S	G	G	NH	NH	NH	NH
GC[b]	UK 711778	UK 293431	UK 293431	UK 293431	UK 293431	UK 400459	TK 876959	TK 876959	TK 876959	TK 876959	TK 935938	TK 935938	UL 000009	UK 911042	UK 911042	TK 787975	TK 787975	TK 787975	TK 908928	TK 908928	TK 890979	TK 890979	TK 890979	TK 890979
Rock type	Q-Diorite	Gabbro	Gabbro	Gabbro	Gabbro	Q-Gabbro	Gabbro	Gabbro	Q-Diorite	Q-Diorite	Gabbro	Gabbro	Q-Diorite	Gabbro	Q-Diorite	Q-Diorite	Gabbro	Gabbro	Gabbro	Gabbro	Gabbro	Gabbro	Gabbro	Q-Diorite
SiO_2	54.34	48.01	48.30	48.77	49.26	51.65	46.60	49.99	52.38	53.14	46.88	47.22	55.87	50.60	54.96	47.38	47.93	48.63	49.34	54.13	49.42	49.68	49.89	58.13
TiO_2	0.71	0.81	0.82	0.98	0.88	0.82	0.75	1.15	1.37	1.18	0.86	0.87	0.64	0.75	1.48	1.53	0.72	1.09	0.63	0.82	0.78	0.75	0.95	1.16
Al_2O_3	17.83	15.68	15.90	14.17	16.18	15.86	14.30	15.15	16.15	16.92	14.97	17.46	18.72	9.41	17.67	16.55	17.66	18.35	14.64	15.60	17.66	18.12	18.40	16.74
Fe_2O_3[c]	7.17	10.21	9.79	10.78	9.53	8.74	11.53	10.96	9.52	8.63	11.64	9.78	6.95	12.04	7.75	9.56	8.89	8.88	10.17	8.06	8.43	7.80	8.43	7.22
MnO	0.11	0.13	0.13	0.14	0.13	0.12	0.15	0.13	0.13	0.12	0.14	0.12	0.09	0.14	0.11	0.14	0.15	0.16	0.15	0.14	0.13	0.13	0.13	0.13
MgO	6.25	13.42	12.45	13.36	11.62	9.98	13.73	10.74	7.04	6.67	14.50	11.00	5.78	18.71	4.30	7.91	12.30	9.65	13.70	9.14	10.25	9.91	8.62	3.67
CaO	8.37	7.42	8.05	7.50	7.69	6.45	5.89	6.24	6.93	6.98	6.39	7.74	6.24	3.47	6.19	8.00	8.86	9.37	7.46	7.50	8.88	9.10	8.78	6.13
Na_2O	2.46	2.41	2.36	2.24	2.48	2.15	2.16	2.67	3.16	3.06	2.18	2.54	2.35	1.41	3.07	2.88	2.49	2.87	2.07	2.36	2.82	2.73	3.07	3.23
K_2O	1.36	0.87	0.73	0.77	0.83	1.34	1.44	1.53	1.76	2.00	0.94	0.81	2.00	1.90	2.40	2.72	0.38	0.49	1.05	1.21	0.58	0.57	0.64	2.71
P_2O_5	0.11	0.10	0.13	0.12	0.12	0.12	0.16	0.25	0.29	0.27	0.19	0.16	0.14	0.14	0.54	0.84	0.09	0.13	0.09	0.11	0.10	0.09	0.13	0.31
LOI	1.20	0.80	1.20	1.00	1.10	2.60	3.10	1.00	1.10	0.90	1.20	2.20	1.10	1.10	1.20	1.57	0.58	0.49	1.03	0.79	0.84	0.91	0.64	0.82
Total	99.9	99.9	99.9	99.8	99.8	99.8	99.8	99.8	99.8	99.9	99.9	99.9	99.9	99.7	99.7	99.1	100.1	100.1	100.3	99.9	99.9	99.8	99.7	100.2
Mg#	0.63	0.72	0.72	0.71	0.71	0.69	0.70	0.66	0.59	0.60	0.71	0.69	0.62	0.75	0.52	0.62	0.73	0.68	0.73	0.69	0.71	0.72	0.67	0.50
Ba	234	165	151	161	157	310	267	359	347	331	196	151	368	365	596	1493	111	141	198	242	130	114	142	848
Rb	48.2	27.3	22.8	23.4	25.4	57.4	50.8	52.7	61.8	65.1	28.4	22.1	84.8	82.3	71.8	98.0	7.0	11.0	31.0	47.0	19.0	20.0	23.0	139.0
Cs	3.1	2.3	1.9	1.4	1.9	5.8	7	3.7	3.4	3	6.2	2.9	6.2	4.4	1.9	6.1	0.9	1.4	2.6	3.6	1.7	2.7	2.8	4.4
Sr	202	301	301	261	305	334	332	363	371	364	305	354	344	157	382	1406	357	396	230	223	269	278	281	267
Pb	6.4	3.8	4.5	3.3	5.2	6.1	4.3	3.5	5.1	5.5	3.7	3.6	9.2	4.4	8.5	8.0	4.0	4.0	4.0	6.0	4.0	4.0	4.0	12
Th	3.0	3.3	2.5	3.0	3.1	4.5	5.0	4.5	4.6	5.4	3.3	2.4	11.1	5.0	11.8	3.8	1.0	1.4	2.6	3.7	1.7	1.4	2.0	7.5
U	1.3	0.9	0.4	0.5	0.6	1.5	1.2	1.5	1.8	1.4	0.8	0.8	2.1	1.7	1.6	1.4	0.2	0.2	0.8	1.4	0.6	0.5	0.7	1.8
Zr	83	125	85	94	97	125	103	102	137	119	116	96	118	39	205	502	70	105	64	55	77	76	103	209
Nb	5.3	5.7	4.6	5.2	5.2	4.7	7.6	10.5	11.2	11.7	6.8	6.0	7.2	5.9	13.6	11.7	1.8	3.0	3.5	5.4	2.5	2.3	2.9	13.1
Y	22.8	19.4	20.1	20.9	20.9	24.1	16.9	25.9	36.3	24.2	20.3	18.2	16.4	19.7	31.7	32.9	15.6	24.9	15.9	25.0	17.6	17.5	20.0	26.7
Sc	25	17	21	25	21	25	13	16	23	18	14	14.0	17	14	17	32	22	26	20	27	21	21	20	19
Co	23	62	60	62	54	51	73	61	39	35	76	59	27	87	22	32	48	44	52	35	46	45	41	20
V	193	129	151	180	150	175	96	115	153	126	94	100	181	87	111	242	123	159	127	181	116	117	123	116
Ni	15	297	235	265	326	78	391	266	196	95	242	169	47	667	39	60	220	140	140	80	170	160	110	20
Cr	390	438	438	712	595	609	568	431	315	260	198	233	281	1170	96	160	630	400	690	510	330	330	210	70
Cu	23.7	58.2	39.7	51.0	95.9	27.6	51.0	38.2	32.9	30.8	32.6	29.5	28.1	68.8	26.5	60.0	40.0	40.0	30.0	20.0	70.0	50.0	40.0	20.0
Zn	34	32	28	28	23	34	47	26	44	47	28	22	58	32	70	120	70	80	90	90	60	70	60	100
Ga	18.8	15.2	15.6	14.5	15.9	18.8	14.9	16.2	19.7	19.9	15.0	15.8	21.9	12.2	18.7	24.0	12.0	16.0	14.0	16.0	15.0	15.0	17.0	23.0
Ta	0.3	0.3	0.2	0.2	0.2	0.3	0.5	0.7	0.8	0.7	0.4	0.5	0.6	0.5	0.9	0.8	0.1	0.2	0.3	0.5	0.2	0.2	0.2	1.0
Hf	2.7	3.3	2.6	2.7	3.3	3.0	2.6	3.3	4.2	3.5	3.3	2.7	3.4	1.4	5.7	11.8	1.6	2.5	1.8	1.7	2.0	1.8	2.5	5.3
La	14.7	13.6	12.4	12.8	13.3	20.0	15.5	20.4	24.7	23.5	17.2	12.5	31.0	14.4	49.1	54.6	5.7	8.8	9.2	12.3	7.3	6.5	8.3	36.7
Ce	31.0	30.2	27.3	28.7	29.1	40.8	32.4	46.6	58.1	50.8	37.2	27.1	62.5	34.6	104.0	122.0	13.6	21.1	19.6	28.5	17.2	15.1	19.3	73.7
Pr	4.02	3.70	3.55	3.65	3.78	5.03	3.98	5.98	7.46	6.07	4.54	3.53	7.46	4.62	13.30	15.10	1.72	2.77	2.32	3.66	2.15	1.93	2.41	8.25
Nd	16.9	13.6	14.4	14.5	14.9	20.5	16.5	24.8	32.2	23.0	18.0	13.5	27.0	19.6	53.1	61.9	8.1	12.3	10.2	17.0	9.8	8.9	10.9	33.5
Sm	3.60	3.21	3.40	3.70	3.82	4.50	3.50	5.39	6.90	4.71	4.10	3.30	4.81	4.30	9.50	10.70	1.99	3.21	2.46	4.18	2.40	2.25	2.68	6.78
Eu	1.03	1.02	1.14	1.07	1.11	1.20	1.05	1.32	1.74	1.27	1.09	1.08	1.57	0.60	1.70	2.43	0.84	1.23	0.84	1.01	0.95	0.86	0.97	1.53
Gd	3.81	3.36	3.70	3.62	3.50	4.27	3.13	5.12	7.25	4.78	3.83	3.36	3.57	3.89	7.61	8.02	2.34	3.82	2.74	4.68	2.88	2.69	3.16	6.26
Tb	0.61	0.49	0.62	0.55	0.59	0.67	0.52	0.79	1.06	0.74	0.56	0.50	0.54	0.62	1.11	1.05	0.41	0.66	0.48	0.77	0.50	0.46	0.53	0.91
Dy	3.79	3.14	3.48	3.54	3.69	3.80	2.97	4.49	6.13	3.97	3.58	2.99	2.74	3.75	5.86	5.84	2.61	4.07	2.83	4.46	3.03	2.83	3.22	4.76
Ho	0.71	0.61	0.68	0.70	0.66	0.74	0.57	0.90	1.19	0.80	0.62	0.57	0.47	0.70	1.03	1.07	0.53	0.83	0.55	0.84	0.61	0.57	0.66	0.88
Er	2.20	1.87	1.97	2.04	2.07	2.38	1.56	2.46	3.40	2.30	1.89	1.80	1.49	1.85	2.93	3.11	1.61	2.44	1.62	2.38	1.79	1.71	1.98	2.42
Tm	0.33	0.28	0.28	0.30	0.30	0.34	0.20	0.34	0.44	0.34	0.25	0.23	0.23	0.26	0.42	0.45	0.25	0.37	0.26	0.35	0.27	0.27	0.30	0.34
Yb	2.02	1.67	1.57	1.87	1.91	2.36	1.44	2.16	2.81	1.99	1.66	1.55	1.40	1.60	2.61	2.87	1.65	2.40	1.66	2.18	1.73	1.74	1.94	2.11
Lu	0.33	0.33	0.27	0.32	0.29	0.36	0.28	0.33	0.50	0.36	0.28	0.26	0.25	0.28	0.36	0.44	0.23	0.35	0.24	0.31	0.26	0.24	0.31	0.29

[a]B: Becedillas, BE: Berrocal; G: Gallegos; MA Martínez; ME: Mercadillo; NH: Navahermosa; NM: Navamorcuende; S: La Solanilla; TA: Talavera; TI: El Tiemblo. [b]GC: Geographic co-ordinates; all samples are within the 30 T zone of the Universal Transverse Mercator co-ordinate system, excepting those from Talavera massif which are in the 30 S zone. [c]Total Fe expressed as Fe_{2O3}.

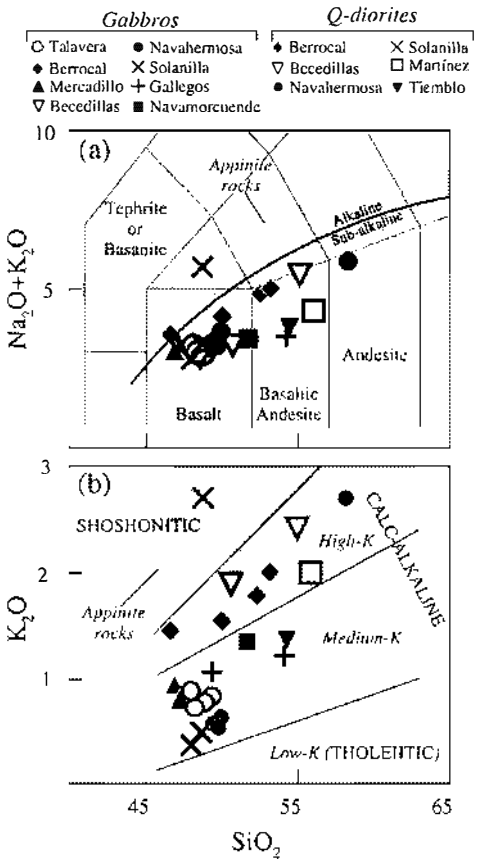

Fig. 4. Total alkalies vs silica diagram of Le Bas et al. (1986) (a) and K_2O vs SiO_2 plot with shoshonitic and low-K to high-K fields after Peccerillo and Taylor (1976) (b) for the SCS gabbroic and quartzdioritic intrusions. The line separating alkaline and subalkaline domains in diagram (a) and the appinite compositional field are taken, respectively, from Irvine and Baragar (1971) and Bowes and Košler (1993).

some degree of differentiation must have occurred. Given that the samples were collected from different gabbroic intrusions, the possible influence of a crystal fractionation process might be evaluated considering the Berrocal outcrop, which is represented by four samples with a continuous variation from Mg-rich gabbro to quartzdioritic terms. Mg, Fe, Mn, Cr and Ni contents decrease towards more differentiated compositions, which might be taken as an evi Cr-spinel, whereas the other major (Si, Ti, Al, Ca, Na, K) and trace (e.g., Rb, Sr, Th, U, Nb, Ta, REE) elements increase their concentrations in the more evolved rocks. Furthermore, mineral major element contents also have a wide compositional range, in accordance with the occurrence of a fractionation process. Mineral zoning, such as that developed by plagioclase towards Ab-rich rims, also supports this idea.

Similar ages of basic and acid Variscan magmatism, together with field evidence of local mingling between both magma types (e.g., ocellar quartz and granite enclaves in quartzdiorites), suggest that granite hybridization was an important factor in the evolution of some of the studied gabbroic intrusions (e.g., Navahermosa outcrop). Moreover, the large isotopic variation in the La Solanilla outcrop (unrelated to granites) suggests assimilation/contamination with the metamorphic wall rocks.

The contamination or hybridization of a basic magma with crustal-derived materials should be reflected in their isotopic ratios. The Sr–Nd radiogenic composition of quartzdiorites from the Navahermosa and La Solanilla intrusions exhibits a moderate enrichment when compared with the associated Mg-rich primitive gabbros (Fig. 7). To test the relevance of hybridization processes in their genesis, we used these intrusions because they show the most contrasting isotopic composition between the basic and intermediate rocks. We estimated the degree of mixing or assimilation using Assimilation and Fractional Crystallization (AFC) models. Magma mixing can be accompanied with concurrent crystal fractionation in the higher-T basic melt. Thus, AFC modelling could be used to evaluate mixing processes in gabbroic melts (e.g. Dias and Leterrier, 1994). To quantify the degree of magma mixing or assimilation involved we have considered the Variscan SCS granites and the host metapelites as crustal end-members (see input data in Fig. 9 caption). The quartzdiorites from Navahermosa massif show clear evidence of granite magma mixing, which is in accordance with the geochemical variation within this intrusion: εNd is positively correlated to Mg# and negatively correlated to Rb/Sr and SiO_2 (Fig. 9). The results of the AFC model for this massif are based on two different hybridization/fractionation (r) values. Magma mixing rates close to 18% would be required to reach Rb/Sr ratios similar to those of sample 108604 (Navahermosa) when $r=0.5$ (Fig. 9c). On the other hand, La Solanilla massif intrudes metapelitic migmatites, and no evidence of magma mixing with granitic intrusives has been observed. The AFC model supports 7% assimilation of metapelitic rocks for $r=0.4$. Additionally, the geochemical variation shown by samples from the Mercadillo intrusion (also emplaced within metamorphic rocks) is in accordance with a similar process of wall-rock assimilation (Fig. 9c).

6.2. Nature of the mantle sources

A discussion on the mantle sources should only consider those samples without textural or chemical evidence of hybridization processes. Although some of the studied outcrops (Navahermosa, La Solanilla and Mercadillo) have evolved rocks implying open-system processes, the accompanying primitive gabbros do not show petrographic or geochemical evidence to suggest that these processes were involved in their genesis. These Mg-rich gabboric samples (108038 and 108039 from Talavera; 108585 and 108588 from La Solanilla; 108599 and 108601 from Navahermosa; 107055 from Mercadillo; 107053 from Berrocal; and 108595 from Gallegos) most probably represent the most basic and uncontaminated rocks of these intrusions. The isotopically most enriched primitive gabbros (Talavera and Gallegos) show low contents in trace elements which are typically enriched in the continental crust (e.g., Th, U, K or Rb; Fig. 5), that do not support significant crustal contamination during magma transport and emplacement. Thus, their isotopic composition represents that of the mantle source prior to magma generation.

The Mg-rich SCS gabbros show differences in their isotopic and major and trace element composition (Figs. 5, 7 and 8). However, the dence contrasting compositions defined on the basis of the trace and major element contents (e.g., K, Rb, U, and Ca; see Fig. 5) disagree with that indicated by the isotopic ratios. Accordingly, some chemical differences might be ascribed to source heterogeneities such as variable proportions of K-bearing minerals in the mantle (e.g., phlogopite).

Chondrite-normalised LREE abundances in the Mg-rich SCS gabbros are variable (e.g., $La_N=24$–86), and the LILE show similar trends. However, the trace element normalised patterns are very similar for the whole group of samples (Fig. 6). By contrast, the HREE chondrite-normalised values are fairly homogeneous and poorly fractionated ($Sm/Yb_N=1.3$–2.8). These moderate ratios suggest that partial melting occurred in the stability field of spinel, although garnet could also be present in the mantle source (Fig. 10).

In addition to the LILE and LREE enrichment, a metasomatic process in the mantle source is required to account for the negative P anomaly (Fig. 6) and the presence of relatively abundant primary hydrous phases (phlogopite, amphibole) in the SCS gabbros. This requires the presence of a residual P-bearing phase (e.g., apatite) in the mantle source and the participation of some hydrated mineral during partial melting.

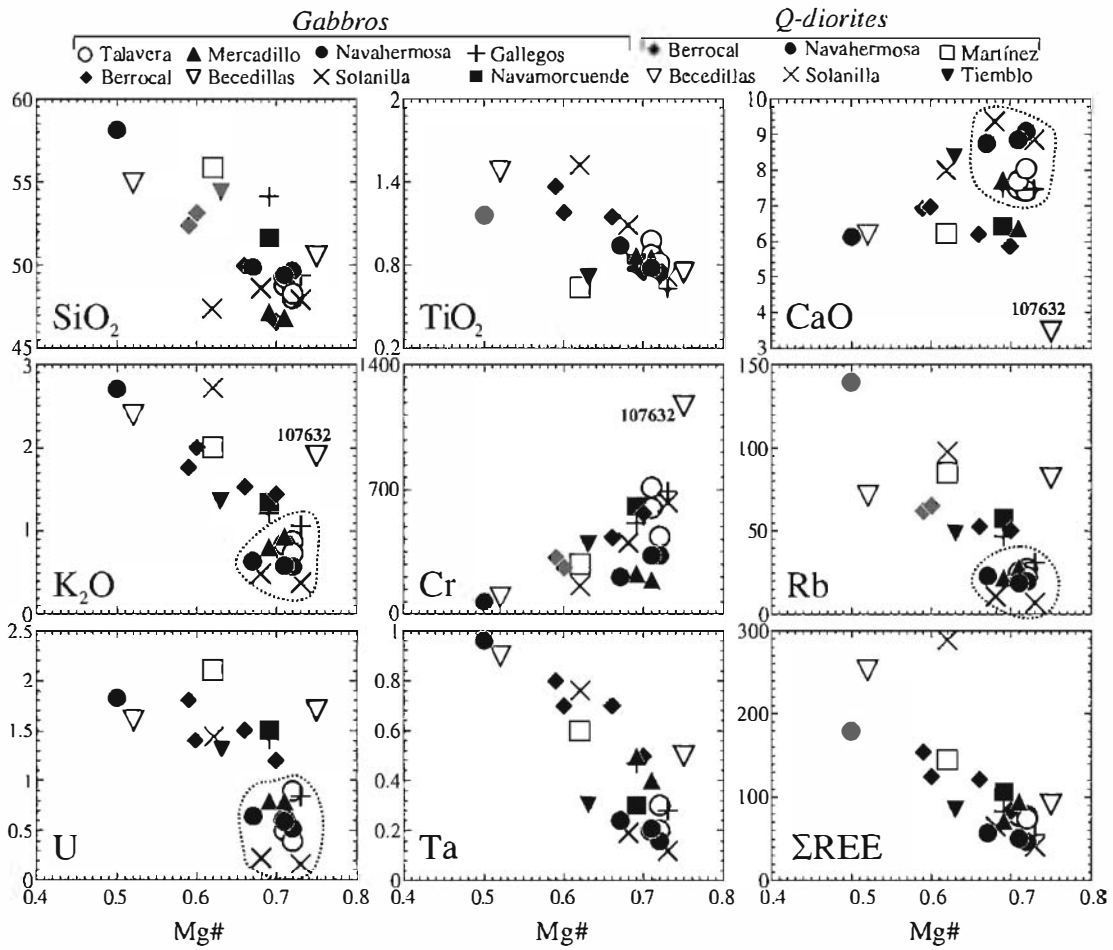

Fig. 5. Whole-rock chemistry of the SCS gabbroic and quartzdioritic intrusions. Major and trace element contents expressed in wt.% and ppm, respectively. The field encircled by the dotted line highlights a group of rocks with a slightly different composition (see explanation in the text). The amph-rich gabbro 107632 plots outside the SCS gabbros field in some diagrams.

The primitive mantle-normalised multi-element plots of these Mg-rich gabbros show typical arc-like trace element patterns (LILE enrichment and deep Nb, Ta and Ti troughs), together with large positive Pb anomalies (Fig. 6). Their incompatible trace element ratios, such as Th/Yb (0.5–2.1), Ta/Yb (0.07–0.32), Ce/Pb (mainly 3.4–13.3) and Ba/Nb (mainly 25–62), are similar to those of the continental crust (Rudnick and Fountain, 1995; Rudnick and Gao, 2003), and resemble the values recorded by magmas that formed in active continental margins (Wilson, 1989). Taking into account these data, the involvement of a crustal-derived or subduction-modified component in the mantle sources is apparent.

The SCS gabbroic and granitic magmas correspond to late intrusions during the Variscan orogeny, which occurred in the Central Iberian Zone (the innermost part of the Variscan collisional belt). This magmatism developed in an extensional tectonic setting (Dobłas et al., 1994), more than 50 Ma after the continental collision had ended (e.g., Azor et al., 1994; Villaseca and Herreros, 2000). The involvement of oceanic lithosphere subduction is doubtful. The nearest possible location of oceanic crust was the south-western Central Iberian Zone boundary, adjacent to the Ossa–Morena Zone, which has been considered to be a suture zone (Matte, 1986; Azor et al., 1994; Simancas et al., 2001). Amphibolite rocks from this suture contact have been used as evidence that oceanic materials from the Ossa–Morena Zone were accreted beneath the Central Iberian Zone in this region during the Devonian (Gómez-Pugnaire et al., 2003). However, in either case, oceanic accretion is likely to have been located more than 300 km to the south of the SCS. There is no geologic evidence relating the Central Iberian Zone to oceanic subduction during Variscan time and volcanism in this realm from Ordovician to Devonian was intraplate, of alkaline geochemical affinity, and mainly basaltic in composition (e.g., Higueras et al., 2001; Gutiérrez-Alonso et al., 2008).

Thus, recycling of continental crustal components into the mantle can be considered as a plausible hypothesis to account for the geochemical and isotopic signatures of the SCS primitive gabbros. This process, which implies the incorporation of lower/middle crustal materials, has been proposed for the European Variscan Belt by several authors (e.g., Turpin et al., 1988; Becker et al., 1999; Lustrino et al., 2000; Monjoie, 2004; Massonne, 2005) to explain the genesis of post-collisional gabbroic, pyroxenitic and mafic volcanic rocks.

The involvement of a crustal Sr–Nd enriched component within the mantle should be reflected in the isotopic ratios of the SCS primitive gabbros. Their $^{87}Sr/^{86}Sr$ and εNd radiogenic values show a significant variation from 0.7041 to 0.7056 and from +3.1 to −1.6, respectively. This compositional range yields a negative correlation (Fig. 7), which might involve the incorporation of a radiogenic component in the mantle source. We have modelled such a process considering lower crustal metaigneous and metasedimentary protoliths as potential sources for a hypothetical mixed crustal component. The SCS primitive gabbros isotopic variation fits well with a mixing model involving the recycling of a lower crustal component, whereas the orthogneissic and metapelitic rocks from SCS granulite terrains, which represent middle crustal materials, are significantly enriched in radiogenic Sr (Fig. 11). The SCS lower crust isotopic composition has

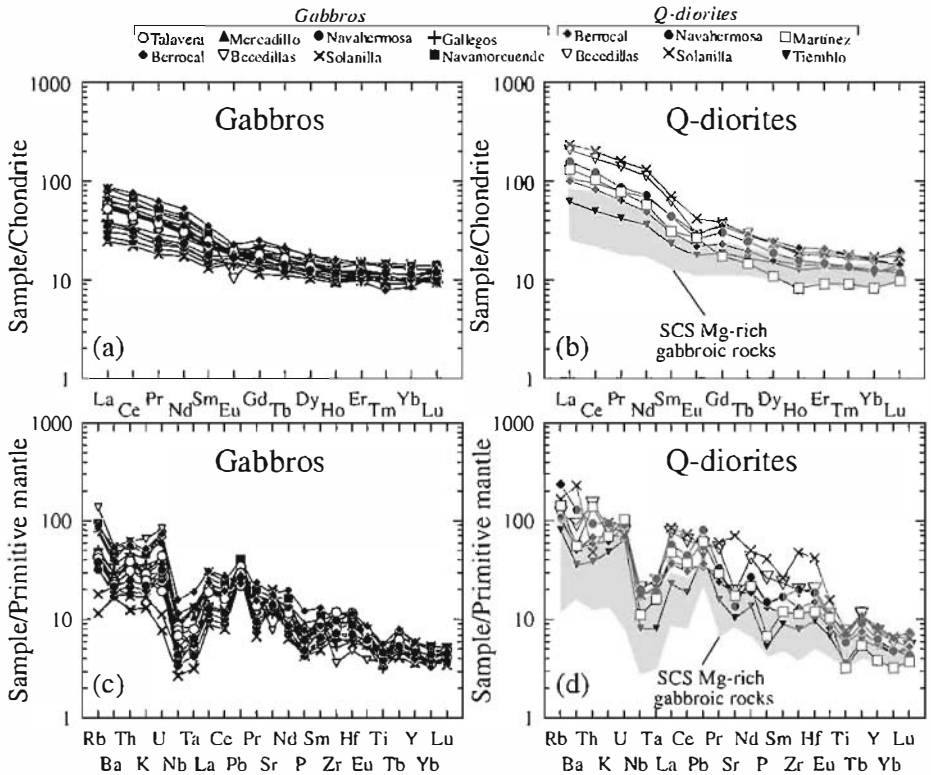

Fig. 6. Chondrite and primitive mantle-normalised trace element composition of the SCS gabbroic (a, c) and quartzdioritic (b, d) intrusions. Normalising values after Sun and McDonough (1989) and McDonough and Sun (1995), respectively.

been estimated from the deep-seated granulitic xenoliths carried by SCS Permian ultrabasic alkaline dykes (Villaseca et al., 1999, 2007), which display equilibrium pressures in the range 0.7–1.1 GPa. Three different types of lower crustal granulites have been distinguished in the Spanish Central System: 1) felsic peraluminous metaigneous granulites, 2) metapelitic granulites and, 3) charnockitic granulites. Charnockite xenoliths have Sr–Nd radiogenic values similar to those of the SCS gabbros, thus they cannot account for the isotopic heterogeneity in the gabbros. Accordingly, we have modelled a mixing process involving an originally depleted mantle source and two distinct lower crustal components (see model parameters in Fig. 11 caption). The latter involves the composition of the felsic and pelitic granulites after Villaseca et al. (1999). The initial mantle component used in the model is isotopically similar to the most depleted SCS gabbros. The model fits better if only the pelitic granulites are considered (Fig. 11). Thus, the mixing of a peridotitic upper mantle with about 1–2% of subducted continental materials geochemically similar to metapelitic granulites adequately accounts for the Sr–Nd isotopic composition of the SCS gabbroic intrusions (Fig. 11).

Such crustal influence is also reflected in the incompatible trace element ratios shown by these primitive gabbros. Fig. 12 shows the composition of the most primitive SCS gabbros and a mixing model calculated for εNd and Ba/Nb–Th/Yb ratios. As explained above, the two components used in the model are the lower crustal metapelitic xenoliths and the most $^{144}Nd/^{143}Nd$-depleted gabbros. Similarly, the

Table 3
Sr–Nd isotopic composition of the SCS gabbroic intrusions.

Sample	Rock type	Location[a]	Rb (ppm)	Sr (ppm)	$^{87}Rb/^{86}Sr$	$^{87}Sr/^{86}Sr \pm (2\sigma)$	$^{87}Sr/^{86}Sr_{305\ Ma}$	Sm (ppm)	Nd (ppm)	$^{147}Sm/^{144}Nd$	$^{143}Nd/^{144}Nd \pm (2\sigma)$	$\varepsilon(Nd)_{305\ Ma}$
107038	Gabbro*	TA	23.4	261	0.26	0.706692 ± 06	0.70556	3.7	14.5	0.154	0.512471 ± 03	−1.6
107039	Gabbro*	TA	27.3	301	0.26	0.706702 ± 06	0.70556	3.2	13.6	0.142	0.512449 ± 03	−1.6
107048	Q-gabbro	NM	57.4	334	0.50	0.708627 ± 05	0.70647	4.5	20.5	0.133	0.512392 ± 03	−2.3
107053	Gabbro*	BE	52.7	363	0.42	0.706470 ± 06	0.70464	5.4	24.8	0.132	0.512525 ± 03	0.3
107057	Gabbro	ME	28.4	305	0.27	0.706356 ± 05	0.70518	4.1	18.0	0.138	0.512435 ± 03	−1.7
107055	Gabbro*	ME	22.1	354	0.18	0.705468 ± 04	0.70468	3.3	13.5	0.148	0.512574 ± 03	0.7
107632	Gabbro	B	82.3	157	1.52	0.712619 ± 06	0.70603	4.3	19.6	0.133	0.512376 ± 03	−2.6
108599	Gabbro*	NH	20.0	278	0.21	0.705301 ± 07	0.70440	2.3	8.9	0.152	0.512618 ± 03	1.3
108601	Gabbro*	NH	23.0	281	0.24	0.705205 ± 06	0.70418	2.7	10.9	0.149	0.512633 ± 03	1.8
108604	Q-diorite	NH	139	267	1.51	0.713299 ± 06	0.70676	6.8	33.5	0.122	0.512265 ± 04	−4.4
108585	Gabbro*	S	11.0	396	0.08	0.704401 ± 05	0.70405	3.2	12.3	0.158	0.512685 ± 04	2.4
108588	Gabbro*	S	7.0	357	0.06	0.704543 ± 05	0.70430	2.0	8.1	0.149	0.512667 ± 03	3.1
108591	Q-diorite	S	98.0	1406	0.20	0.706570 ± 05	0.70569	10.7	61.9	0.104	0.512317 ± 03	−2.7
108595	Gabbro*	G	31.0	230	0.39	0.707256 ± 05	0.70556	2.5	10.2	0.146	0.512470 ± 03	−1.3

Rb, Sr, Sm and Nd concentrations determined by ICP-MS. [a]B: Becedillas, BE: Berrocal, G: Gallegos, ME: Mercadillo, NH: Navahermosa, NM: Navamorcuende, S: La Solanilla, TA: Talavera.
*The most Mg-rich gabbros, considered for the petrogenesis discussion.

Table 4
Pb isotopic composition of the SCS gabbroic intrusions[a].

Sample	107038	107039	107048	107053	107057	107055	107632
Location[b]	TA	TA	NM	BE	ME	ME	B
$^{206}Pb/^{204}Pb$	18,547	18,353	18,347	18,263	18,283	18,346	18,254
$^{207}Pb/^{204}Pb$	15.630	15,633	15,637	15,614	15,634	15,645	15,632
$^{208}Pb/^{204}Pb$	38,837	38.400	38,317	38,215	38,356	38,377	38,257

[a] Pb isotopic data have been determined on feldspar separates, thus the measured ratios may be considered the initial values at the age of magma formation.
[b] B: Becedillas, BE: Berrocal, ME: Mercadillo, NM: Navamorcuende, TA: Talavera.

increasing Th/Yb and decreasing Ba/Nb ratios of the olivine gabbros fit well with a low degree of mixing (~2%) of deep pelitic metasediments within the mantle (Fig. 12).

The presence of dense, highly restitic metapelitic granulites (ρ~3.1–3.7 g/cm^3; Villaseca et al., 1999) would facilitate lower crustal delamination or continental subduction. Even though the nature of this component may be unclear, a main conclusion from this study is the involvement of a recycled component into the mantle, which might be associated with lower crustal material. Such an enrichment event accounts for the arc-like signatures of these mantle-derived rocks and explains the addition of volatiles to the mantle source. The Pb isotope ratios of the SCS gabbroic rocks resemble those of the SCS granulite xenoliths (Villaseca et al., 2007) (Fig. 8). These values represent the influence of an enriched material in the upper mantle, which has been also recorded in the SCS Permian alkaline dykes, and related to an EMII-like component (Orejana et al., 2008). The fact that the EMII reservoir would be associated with the incorporation of continental crustal rocks into the mantle (Zindler and Hart 1986), further supports our proposals involving either continental subduction or delamination during the Variscan collision.

7. Evolution of the subcontinental lithospheric mantle under central Spain

Mantle-derived magmas in central Spain intruded over a long period of time, from late Variscan to Early Jurassic, thus generating a valuable record for the geochemical characterization of their mantle sources. Following Villaseca et al. (2004), these rocks comprise the Gb1 calc–alkaline gabbroic intrusions studied in this work and the subsequent suites of dyke swarms with calc–alkaline (Gb2), shoshonitic (Gb3), alkaline (Gb4) and tholeiitic (Gb5) geochemical affinities. This magmatic suite records a highly heterogeneous isotopic composition, ranging from near PREMA to $^{87}Sr/^{86}Sr$-enriched radiogenic values (Villaseca et al., 2004 and references therein). The enriched signature shown by these mafic rocks has been attributed to crustal recycling in the source region, crustal assimilation or magma mixing during transport or emplacement at shallower levels, or a combination of these mechanisms. For example, significant contamination is likely to be involved in the genesis of the Gb5 Jurassic Messejana–Plasencia tholeiitic dyke. However, the initial Sr–Nd isotopic signatures of their mantle sources, estimated at a pre-assimilation stage ($^{87}Sr/^{86}Sr$~0.705, $^{143}Nd/^{144}Nd$~0.5124; Cebriá et al., 2003), corresponds to a lithospheric composition (resembling the Bulk Silicate Earth: BSE), that clearly overlaps the compositional field defined by the SCS gabbros. The highest Sr radiogenic ratios recorded by the SCS mafic magmatism (up to 0.7087) are found in the Gb2 calc–alkaline primitive rocks, and have been considered as a possible indication of a crustal recycling process (Villaseca et al., 2004). Basic rocks from other areas within the Iberian Massif show a Sr–Nd composition very similar to those of the SCS gabbros (Fig. 7). Although these rocks are likely to be part of a wider suite involving more silica-rich magmas (by mixing with acid magmas: Galán et al., 1996; Dias et al., 2002; Vilá et al., 2005), the most depleted samples overlap the field represented by the SCS primitive gabbros. Thus, it is likely that trends showing strong

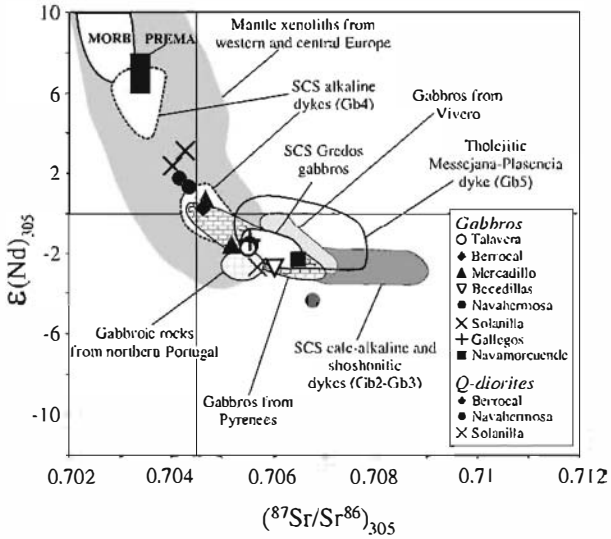

Fig. 7. Initial Sr–Nd isotopic composition of the SCS gabbroic intrusions back-calculated to 305 Ma. The composition of different Variscan or post-Variscan mafic intrusions from central Spain and other regions of the Iberian Massif, together with that of mantle xenoliths from western and central Europe, are also plotted for comparison. The field of SCS Gredos gabbros is from Moreno-Ventas et al. (1995) and Bea et al. (1999); calc–alkaline Gb2–Gb3: Villaseca et al. (2004); alkaline Gb4 suite: Orejana et al. (2008); Messejana-Plasencia tholeiitic dyke: Alibert (1985) and Cebriá et al. (2003); gabbros from Vivero: Galán et al. (1996); gabbroic rocks from northern Portugal: Dias and Leterrier (1994) and Dias et al. (2002); gabbros from Pyrenees: Vilá et al. (2005); mantle xenoliths from western and central Europe: Beccaluva et al. (2004) and references therein. MORB and PREMA fields taken from Wilson (1989) and Zindler and Hart (1986), respectively.

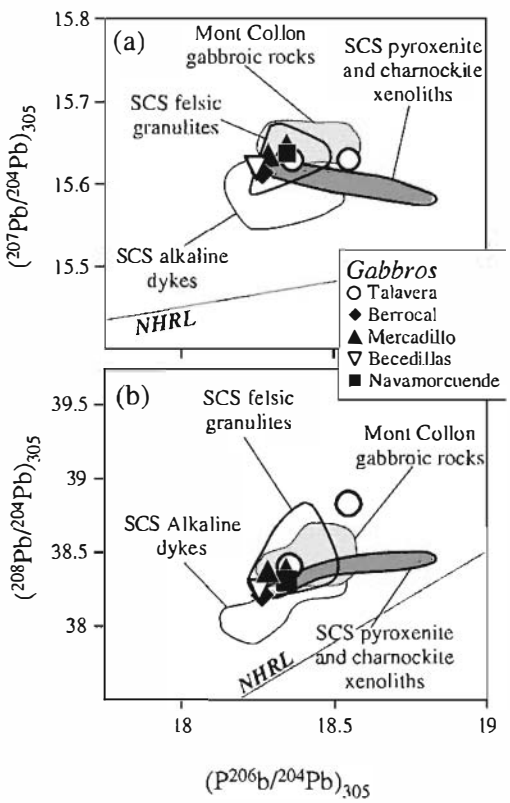

Fig. 8. Initial Pb isotopic composition of the SCS gabbroic intrusions. SCS alkaline dykes: Orejana et al. (2008); SCS felsic granulites and pyroxenitic and charnockitic xenoliths: Villaseca et al. (2007); North Italy (Mont Collon) gabbroic rocks: Monjoie (2004). NHRL: Northern Hemisphere Reference Line.

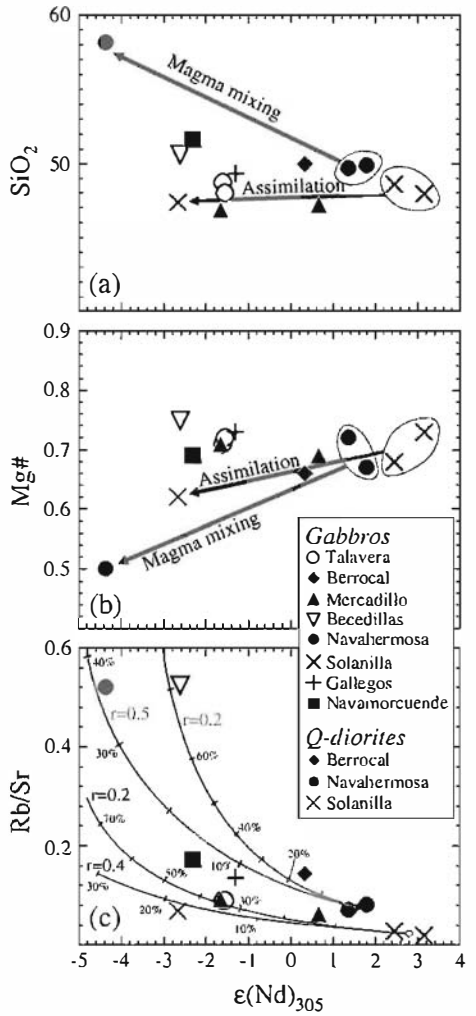

Fig. 9. (a) SiO_2, (b) Mg# and (c) Rb/Sr ratio vs $\varepsilon(Nd)_0$ for the SCS gabbroic intrusions. The arrows in plots (a) and (b) represent the influence of magma mixing and crustal assimilation at shallow levels in the genesis of Navahermosa and La Solanilla massifs, respectively. Plot (c) shows the degree of crystal fractionation in two independent AFC models made for Navahermosa (grey lines) and La Solanilla (black lines). Two contrasting assimilation/fractionation ratios have been considered (0.2 and 0.5 for Navahermosa and 0.2 and 0.4 for La Solanilla). Initial melt compositions: average of samples 108599 and 108601 (Navahermosa), and average of samples 108585 and 108588 (La Solanilla). The composition of the granitic magma mixed with the Navahermosa gabbro corresponds with the averaged values of the Variscan SCS granites (Villaseca et al. 1998): $\varepsilon Nd = -5.7$ and $Rb/Sr = 1.6$. The composition of the assimilated material for La Solanilla gabbro has been taken from averaged SCS metapelites (Villaseca et al., 1998): $\varepsilon Nd = -12$ and $Rb/Sr = 0.96$. The bulk D_{Nd} (0.32), D_{Sr} (0.8) and D_{Rb} (0.08) have been calculated using the following fractionating phases: Plg (50%), Opx (25%), Cpx (15%) and Ol (10%), and the mineral/melt partition coefficients from McKenzie and O'Nions (1991), except D_{Sr} for plagioclase taken from Philpotts and Schnetzler (1970).

enrichment in radiogenic Sr coupled with slight variations in εNd can be ascribed to granite magma mixing, while primitive gabbros plotting on the mantle array reflect heterogeneities within the mantle source.

However, part of the SCS alkaline suite of dykes shows evidence for the input of a depleted sub-lithospheric component, which has been related to the ascent of asthenospheric mantle during widespread rifting around 265 Ma (Villaseca et al., 2004; Orejana et al., 2006, 2008). The existence of a depleted reservoir within the lithospheric mantle beneath central Spain is also supported by data from this work, indicating depleted signatures in the late Variscan gabbros from the Central Iberian Zone (initial εNd up to +3.1). In this respect, we suggest that our potential enriched crustal component would have

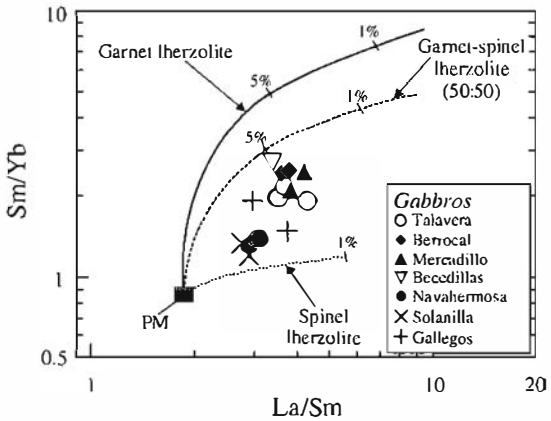

Fig. 10. La/Sm vs Sm/Yb ratios of the SCS Mg-rich gabbros. The plotted lines represent a model for these REE ratios considering a garnet lherzolite, a garnet-spinel lherzolite (with equal proportions of both minerals) and a spinel lherzolite, using the non-modal batch melting equations of Shaw (1970) and primitive mantle as the starting composition. Primitive mantle composition after McDonough and Frey (1989).

mixed within the depleted mantle source. Thus, the lithospheric mantle under central Spain is more heterogeneous than previously thought and expands its composition towards slightly more depleted values.

Many investigations have focused on the study of the mantle xenoliths included within basic or ultrabasic alkaline volcanics from western and central Europe to constrain both the nature and composition of the sub-continental lithospheric mantle and its history of multistage depletion and enrichment events (e.g., Downes and Dupuy, 1987; Beccaluva et al., 2001; Downes, 2001; Downes et al., 2003; Beccaluva et al., 2004; Féménias et al., 2004). According to these works, the Sr–Nd radiogenic composition of the western European lithospheric mantle plots within a wide field from MORB to BSE (Beccaluva et al., 2001). The occurrence of metasomatic enrichment events has been frequently detected in these xenoliths and related to infiltration of different types of incompatible element- and volatile-bearing melts or fluids. This phenomenon may be associated with deep asthenospheric melts (Witt-Eickschen and Kramm, 1998)

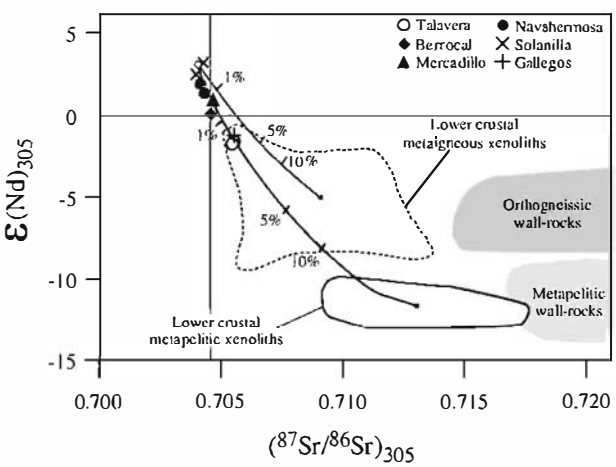

Fig. 11. Mixing models involving a depleted mantle and two different lower crustal components (averaged compositions): felsic granulite and metapelitic xenoliths from the Spanish Central System. Only the Mg-rich primitive SCS gabbros have been plotted (see Table 3). The fields of SCS lower crust granulites are taken from Villaseca et al. (1999). Orthogneissic and metapelitic wall-rocks after Villaseca et al. (1998). Model parameters for the depleted component: $^{143}Nd/^{144}Nd = 0.5128$, Nd = 1.2 ppm, $^{87}Sr/^{86}Sr = 0.7028$, Sr = 11.3 ppm (trace element concentrations after Rehkamper and Hofmann, 1997). Model parameters for the felsic granulites and metapelites, respectively: $^{143}Nd/^{144}Nd = 0.51204$, Nd = 30 ppm, $^{87}Sr/^{86}Sr = 0.709$, Sr = 220 ppm; $^{143}Nd/^{144}Nd = 0.5117$, Nd = 40 ppm, $^{87}Sr/^{86}Sr = 0.713$, Sr = 150 ppm.

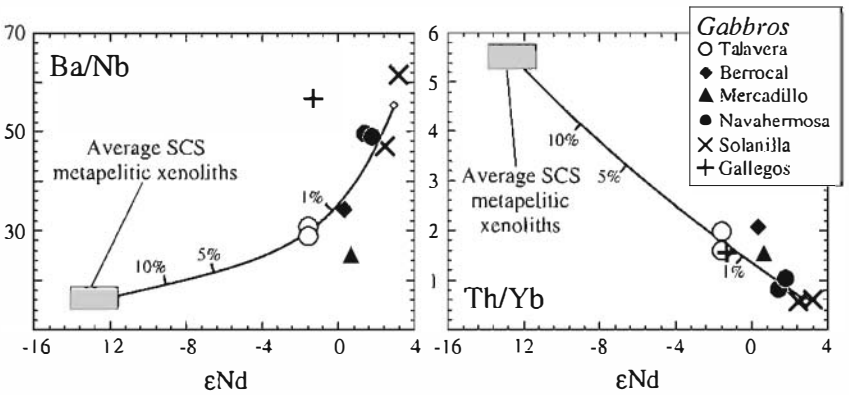

Fig. 12. Mixing model calculated for Ba/Nb and Th/Yb ratios and $\varepsilon(Nd)_0$. Only the most primitive SCS gabbros have been plotted. The starting composition corresponds with an isotopically depleted component similar to the average La Solanilla gabbros ($^{143}Nd/^{144}Nd = 0.51238$, Nd = 10 ppm, Ba/Nb = 55.5; Th/Yb = 0.58). The hypothetic contaminant used represents the average lower crustal SCS metapelitic xenoliths ($^{143}Nd/^{144}Nd = 0.5117$, Nd = 40 ppm, Ba/Nb = 16.3, Th/Yb = 5.5; Villaseca et al., 1999).

although the involvement of isotopically enriched components could be also present (Beccaluva et al., 2001; Wilson and Downes, 1991; Witt-Eickschen et al., 2003). The latter would result in the increase of the $^{87}Sr/^{86}Sr$ ratios, coupled to a decrease in $^{143}Nd/^{144}Nd$. Witt-Eickschen et al. (2003) attribute this enrichment in the Cenozoic Eifel lithospheric mantle to the incorporation of a crustal component during the Variscan orogeny. Similarly, Turpin et al. (1988) suggest that the composition of several Variscan calcalkaline lamprophyres from the Armorican, Central and Voges-Schwarzwald Massifs is in agreement with the recycling of continental crust within the lithospheric mantle. Menzies and Bodinier (1993) pointed out that the western European lithospheric mantle should have evolved in response to repeated cycles of collision-subduction and intraplate extension throughout the Phanerozoic. They also suggest that some Variscan magmas were derived from shallow lithospheric reservoirs containing a metasedimentary component. Metasomatism of the lithospheric mantle by continental crust during Variscan time was also indicated by Becker et al. (1999). Massonne (2005) relates the submersion of dense crustal blocks in the thickened Variscan collisional belt to delamination processes.

The primitive uncontaminated mafic magmas of central Spain have isotopic signatures similar to the composition of the European subcontinental lithospheric mantle (Fig. 7). They are predominantly enriched in radiogenic Sr, which is a geochemical feature that might be associated with the recycling of continental crust. We propose that biotite breakdown melting reactions occurring on lower crustal metaigneous or metapelitic materials may have induced formation of highly restitic granulites, which could have promoted lower crustal delamination and a subsequent mantle metasomatism. In turn, recycling of this component would result in heterogeneous isotopic compositions such as those recorded by the multistage SCS basic magmatism. Whether this recycling took place during the Variscan collision or in previous orogenic cycles is a matter that goes beyond the scope of this work.

The Pb isotopic data of the SCS basic intrusives overlap the wide field of peridotites from the European sub-continental mantle (Downes, 2001, and references therein). Downes (2001) suggests that two trends of radiogenic Pb enrichment may be distinguished in these xenoliths: 1) an increase of $^{206}Pb/^{204}Pb$ and $^{207}Pb/^{204}Pb$ related to participation of a HIMU reservoir, and 2) a relative increase in $^{207}Pb/^{204}Pb$ without a significant modification of the $^{206}Pb/^{204}Pb$ ratios, which could be related to subduction derived agents. The composition of the SCS basic rocks does not fit the first possibility, because they have moderate to high values of $^{207}Pb/^{204}Pb$ and $^{208}Pb/^{204}Pb$ with respect to those of the $^{206}Pb/^{204}Pb$ ratios (close to the PREMA-like isotopic signature) (Fig. 8). This type of enriched composition does not fit either an EM-I component (whose features include very low $^{206}Pb/^{204}Pb$), but would be in agreement with a derivation from an EM-II reservoir (whose composition is thought to resemble that of terrigenous sediments; Hofmann, 2003 and references therein). The difference in Pb concentration between the continental crust and mantle rocks is much greater than that of Sr and Nd. This implies that the Pb isotopic composition of a contaminated mantle source is shifted more readily towards the crustal value than either the Sr or Nd radiogenic values (Rudnick and Goldstein, 1990). This could explain the similarity in the Pb radiogenic compositions between the SCS basic mantle-derived rocks and the lower crustal granulite xenoliths (Fig. 8).

8. Conclusions

A scarce volume of basic to intermediate magmas (mostly coeval with the huge granitic magmatism) intruded in the SCS at the end of the Variscan orogeny. Mineral and whole-rock major and trace element compositional variations are in agreement with a crystal fractionation process conditioned by crystallization of Cr-spinel and olivine.

Although crustal contamination and granite magma mixing are likely to be important factors controlling the composition of the most differentiated samples, the most primitive SCS gabbros do not show variation in the Sr–Nd isotopic signatures or Rb/Sr ratio with increasing SiO_2, which implies the absence of significant assimilation or hybridization with felsic crustal rocks.

The trace element composition of the SCS gabbroic intrusions is characterised by an enrichment of LILE, LREE and Pb coupled to strong Nb–Ta–Ti depletion. Given that no geologic evidence supports oceanic plate subduction during late Variscan time in central Iberia, this geochemical signature is likely to be related to metasomatism of the sub-continental lithospheric mantle via crustal recycling. Models based on the incompatible trace elements and Sr–Nd radiogenic ratios support a minor contamination (~2%) and suggest that the source enrichment might be the granulitic lower crust (probably of metapelitic nature).

The Sr–Nd isotopic composition of the lithospheric mantle under central Spain ranges from slightly depleted to variably enriched, and is very similar to that of the mantle xenoliths recorded from Permian to Cenozoic volcanic materials from western and central Europe. This fact suggests that crustal components were recycled during the Variscan or prior orogenies and variably mixed with a depleted mantle.

Acknowledgements

We acknowledge Alfredo Fernández Larios and José González del Tánago for their assistance with the electron microprobe analyses in the CAI of Microscopía Electrónica (UCM); also José Manuel Fuenlabrada Pérez and José Antonio Hernández Jiménez from the CAI of Geocronología y Geoquímica (UCM) for their help with the Sr–Nd isotopic analytical work by TIMS. We thank the detailed revision made by J.H. Scarrow, an anonymous reviewer and A.C. Kerr, which greatly improved the quality of the manuscript. The SYNTHESYS European Union-funded Integrated Infrastructure Initiative grant has allowed us to carry out the Pb isotope analyses at the Swedish Museum of Natural History. This work is included in the objectives of, and supported by, the CGL-2008-05952 project of the Ministerio de Educación y Ciencia of Spain and the CCG07-UCM/AMB-2652 project of the Complutense University of Madrid.

References

Alibert, C., 1985. A Sr–Nd isotope and REE study of Late Triassic dolerites from the Pyrenees (France) and the Messejana dyke (Spain and Portugal). Earth and Planetary Science Letters 73, 81–90.

Azor, A., González Lodeiro, F., Simancas, J.F., 1994. Tectonic evolution of the boundary between the Central Iberian and Ossa–Morena Zones (Variscan Belt, SW Spain). Tectonics 13, 45–61.

Barbero, L., Rogers, G., 1996. Geochemical and isotopic (Sr, Nd) constraints on the origin of the calc–alkaline syn-orogenic association from the Anatectic Complex of Toledo (Hercynian Iberial Belt). Geogaceta 20, 703–706.

Barbero, L., Villaseca, C., Ardonaegui, P., 1990. On the origin of the gabbro-tonalite-monzogranite association from Toledo area (Iberian Hercynian Belt). Schweizerische Mineralogische und Petrographische Mitteilungen 70, 207–219.

Bea, F., 2004. La naturaleza del magmatismo de la Zona Centroibérica: consideraciones generales y ensayo de correlación. In: Vera, J.A. (Ed.), Geología de España. SGE-IGME, Madrid, pp. 128–133.

Bea, F., Montero, P., Molina, J.F., 1999. Mafic precursors, peraluminous granitoids, and late lamprophyres in the Avila batholith; a model for the generation of Variscan batholiths in Iberia. Journal of Geology 107, 399–419.

Bea, F., Montero, P., Zinger, T., 2003. The nature, origin, and thermal influence of the granite source layer of Central Iberia. Journal of Geology 111, 579–595.

Bea, F., Montero, P.G., González-Lodeiro, F., Talavera, C., Molina, J.F., Scarrow, J.H., Whitehouse, M.J., Zinger, T., 2006. Zircon thermometry and U–Pb ion-microprobe dating of the gabbros and associated migmatites of the Variscan Toledo anatectic complex, central Iberia. Journal of the Geological Society of London 163, 847–855.

Beard, J.S., 1986. Characteristic mineralogy of arc-related cumulate gabbros: implications for the tectonic setting of gabbrolic plutons and for andesite genesis. Geology, 14, 848–851.

Beccaluva, L., Bianchini, G., Coltorti, M., Perkins, W.T., Siena, F., Vaccaro, C., Wilson, M., 2001. Multistage evolution of the European lithospheric mantle: new evidence from Sardinian peridotite xenoliths. Contributions to Mineralogy and Petrology 142, 284–297.

Beccaluva, L., Bianchini, G., Bonadiman, C., Siena, F., Vaccaro, C., 2004. Coexisting anorogenic and subduction-related metasomatism in mantle xenoliths from the Betic Cordillera (southern Spain). Lithos 75, 67–87.

Becker, H., Wenzel, T., Volker, F., 1999. Geochemistry of glimmerite veins in peridotites from Lower Austria — implications for the origin of K-rich magmas in collision zones. Journal of Petrology 40, 315–338.

Berger, J., Féménias, O., Coussaert, N., Mercier, J.C.C., Demaiffe, D., 2007. Cumulating processes at the crust-mantle transition zone inferred from Permian mafic-ultramafic xenoliths (Puy Beaunit, France). Contributions to Mineralogy and Petrology 153, 557–575.

Bowes, D.R., Košler, J., 1993. Geochemical comparison of the subvolcanic appinite suite of the British Caledonides and the durbachite suite of the central European Hercynides: evidence for associated shoshonitic and granitic magmatism. Contributions to Mineralogy and Petrology 48, 47–63.

Casillas, R., 1989. Las asociaciones plutónicas tardihercínicas del sector occidental de la Sierra de Guadarrama, Sistema Central Español, (Las Navas del Marques–San Martín de Valdeiglesias). Petrología, Geoquímica, Génesis y Evolución. PhD Thesis. Universidad Complutense de Madrid, Madrid, pp 316.

Casillas, R., Vialette, Y., Peinado, M., Duthou, J.L., Pin, C., 1991. Âges et caractéristiques isotopiques (Sr, Nd) des granitoïdes de la Sierra de Guadarrama occidentale (Espagne). Abstract Séance Spécialisée de la Société Géologique de France. Mémoire de Jean Lameyre.

Castro, A., Patiño Douce, A.E., Corretgé, L.G., de la Rosa, J., El-Biad, M., El-Hmidi, H., 1999. Origin of peraluminous granites and granodiorites, Iberian massif, Spain: an experimental test of granite petrogenesis. Contributions to Mineralogy and Petrology 135, 255–276.

Cebriá, J.M., López-Ruiz, J., Doblas, M., Martins, L.T., Munha, J., 2003. Geochemistry of the early Jurassic Messejana-Plasencia dyke (Portugal-Spain): implications on the origin of the Central Atlantic Magmatic Province. Journal of Petrology 44, 547–568.

Cesare, B., Rubatto, D., Hermann, J., Barzi, L., 2002. Evidence for late Carboniferous subduction-type magmatism in mafic-ultramafic cumulates of the SW Tauern window (Eastern Alps). Contributions to Mineralogy and Petrology 142, 449–464.

Claeson, D.T., Meurer, W.P., 2004. Fractional crystallization of hydrous basaltic "arc-type" magmas and the formation of amphibole-bearing gabbroic cumulates. Contributions to Mineralogy and Petrology 147, 288–304.

Dias, G., Leterrier, J., 1994. The genesis of felsic-mafic plutonic associations: a Sr and Nd isotopic study of the Hercynian Braga Granitoid Massif (Northern Portugal). Lithos 32, 207–223.

Dias, G., Simões, P.P., Ferreira, N., Leterrier, J., 2002. Mantle and crustal sources in the genesis of late-Hercynian granitoids (NW Portugal): geochemical and Sr–Nd isotopic constraints. Gondwana Research 5, 287–305.

Doblas, M., López Ruiz, J., Oyarzun, R., Sopeña, A., Sánchez Moya, Y., Hoyos, M., Capote, R., Hernández Enrile, J.L., Lillo, J., Lunar, R., Ramos, A., Mahecha, V., 1994. Extensional tectonics in the central Iberian Peninsula during the Variscan to Alpine transition. Tectonophysics 238, 95–116.

Downes, H., 2001. Formation and modification of the shallow sub-continental lithospheric mantle: a review of geochemical evidence from ultramafic xenolith suites and tectonically emplaced ultramafic massifs of western and Central Europe. Journal of Petrology 42, 233–250.

Downes, H., Dupuy, C., 1987. Textural, isotopic and REE variations in spinel peridotite xenoliths, Massif Central, France. Earth and Planetary Science Letters 82, 121–135.

Downes, H., Upton, B.G.J., Handisyde, E., Thirlwall, M.F., 2001. Geochemistry of mafic and ultramafic xenoliths from Fidra (Southern Uplands, Scotland): implications for lithospheric processes in Permo-Carboniferous times. Lithos 58, 105–124.

Downes, H., Reichow, M.K., Mason, P.R.D., Beard, A.D., Thirlwall, M.F., 2003. Mantle domains in the lithosphere beneath the French Massif Central: trace element and isotopic evidence from mantle clinopyroxenes. Chemical Geology 200, 71–87.

Dunn, A.M., Reynolds, P.H., Clarke, D.B., Ugidos, J.M., 1998. A comparison of the age and composition of the Sherburne Dyke, Nova Scotia, and the Messejana Dyke, Spain. Canadian Journal of Earth Sciences 35, 1110–1115.

Féménias, O., Coussaert, N., Berger, J., Mercier, J.C.C., Demaiffe, D., 2004. Metasomatism and melting history of a Variscan lithospheric mantle domain: evidence from the Puy Beaunit xenoliths (French Massif Central). Contributions to Mineralogy and Petrology 148, 13–28.

Fernández, C., Castro, A., De la Rosa, J., Moreno-Ventas, I., 1997. Rheological aspects of magma transport inferred from rock structures. In: Bouchez, J.L., Hutton, D.H.W., Stephens, W.E. (Eds.), Granite: From Segregation of Melt to Emplacement Fabrics. Kluver Academic Publishers, Dordrecht, pp. 75–91.

Fernández Suárez, J., Arenas, R., Jeffries, T.E., Whitehouse, M.J., Villaseca, C., 2006. A U–Pb study of zircons from a lower crustal granulite xenolith of the Spanish Central system: a record of Iberian lithospheric evolution from the Neoproterozoic to the Triassic. Journal of Geology 114, 471–483.

Frey, F.A., Green, D.H., Roy, S.D., 1978. Integrated models of basalt petrogenesis: a study of quartz tholeiites to olivine melilitites from south eastern Australia utilizing geochemical and experimental petrological data. Journal of Petrology 19, 463–513.

Galindo, C., Huertas, M.J., Casquet, C., 1994. Cronología Rb–Sr y K–Ar de diques de la Sierra de Guadarrama (Sistema Central Español). Geogaceta 16, 23–26.

Galán, G., Pin, C., Duthou, J.L., 1996. Sr–Nd isotopic record of multi-stage interactions between mantle-derived magmas and crustal components in a collision context. The ultramafic-granitoid association from Vivero (Hercynian Belt, NW Spain). Chemical Geology 131, 67–91.

Gómez Pugnaire, M.T., Azor, A., Fernández-Soler, J.M., López Sánchez-Vizcaíno, V., 2003. The amphibolites from the Ossa–Morena/Central Iberian Variscan suture (Southwestern Iberian Massif): geochemistry and tectonic interpretation. Lithos 68, 23–42.

Gutiérrez-Alonso, G., Murphy, J.B., Fernández-Suárez, J., Hamilton, M.A., 2008. Rifting along the northern Gondwana margin and the evolution of the Rheic Ocean: a Devonian age for the El Castillo volcanic rocks (Salamanca, Central Iberian Zone). Tectonophysics 461, 157–165.

Higueras, P., Oyarzun, R., Morata, D., Munhá, J., 2001. Alkaline mafic magmatism and huge mercury deposits: the Almadén (Ciudad Real, Spain) case. Boletín de la Sociedad Española de Mineralogía 24, 171–172.

Hofmann, A.W., 2003. Sampling mantle heterogeneity through oceanic basalts: isotopes and trace elements. In: Holland, H.D., Turekian, K.K. (Eds.), Treatise on Geochemistry 2. The Mantle and Core. Elsevier Pergamon, Oxford, pp. 61–102.

Irvine, T.N., Baragar, W.R.A., 1971. A guide to the chemical classification of the common volcanic rocks. Canadian Journal of Earth Sciences 8, 523–548.

Leake, B.E., Woolley, A.R., Arps, C.E.S., Birch, W.D., Gilbert, M.C., Grice, J.D., Hawthorne, F.C., Kato, A., Kisch, H.J., Krivovichev, V.G., Linthout, K., Laird, J., Mandarino, J.A., Maresch, W.V., Nickel, E.H., Rock, N.M.S., Schumacher, J.C., Smith, D.C., Stephenson, N.C.N., Ungaretti, L., Whittaker, E.J.W., Youzhi, G., 1997. Nomenclature of amphiboles; report of the subcommittee on amphiboles of the International Mineralogical Association, Commission on New Minerals and Mineral Names. Canadian Mineralogist 35, 219–246.

Le Bas, M.J., Le Maitre, R.W., Streckeisen, A., Zanetin, B.A., 1986. Chemical classification of volcanic rocks based in the total alkali-silica diagram. Journal of Petrology 27, 745–750.

López-Moro, F.J., López-Plaza, M., 2004. Monzonitic series from the Variscan Tormes Dome (Central Iberian Zone): petrogenetic evolution from monzogabbro to granite magmas. Lithos 72, 19–44.

Lustrino, M., Melluso, L., Morra, V., 2000. The role of lower continental crust and lithospheric mantle in the genesis of Plio-Pleistocene volcanic rocks from Sardinia (Italy). Earth and Planetary Science Letters 180, 259–270.

Massonne, H.J., 2005. Involvement of crustal material in delamination of the lithosphere after continent–continent collision. International Geology Review 47, 792–804.

Matte, P., 1986. Tectonics and plate tectonic model for the Variscan Belt of Europe. Tectonophysics 126, 331–334.
McDonough, W.F., Frey, F.A., 1989. REE in upper mantle rocks. In: Lipin, B., McKay, G.R. (Eds.), Geochemistry and Mineralogy of Rare Earth Elements. Mineralogical Society of America, Chelsea, pp. 99–145.
McDonough, W.F., Sun, S.S., 1995. The composition of the Earth. Chemical Geology 120, 223–253.
McKenzie, D., O'Nions, R.K., 1991. Partial melt distributions from inversion of rare earth element concentrations. Journal of Petrology 32, 1021–1091.
Menzies, M.A., Bodinier, J.L., 1993. Growth of the European lithospheric mantle dependence of upper-mantle peridotite facies and chemical heterogeneity on tectonics and age. Physics of the Earth and Planetary Interiors 79, 219–240.
Monjoie, P., 2004. The Mont Collon mafic complex (Austroalpine Dent Blanche nappe): Permian evolution of the western European mantle. PhD Thesis. Université de Lausanne, Lausanne, pp 163.
Montero, P., Bea, F., Zinger, T., 2004. Edad $^{207}Pb/^{206}Pb$ en cristal único de circón de las rocas máficas y ultramáficas del sector de Gredos, batolito de Ávila (sistema central espanol). Revista de la Sociedad Geológica de España 17, 157–167.
Moreno-Ventas, I., Rogers, G., Castro, A., 1995. The role of hybridization in the genesis of the Hercynian granitoids in the Gredos Massif, Spain: inferences from Sr–Nd isotopes. Contributions to Mineralogy and Petrology 120, 137–149.
Orejana, D., Villaseca, C., Billström, K., 2005. A PREMA asthenospheric component for the Permian alkaline dykes of the Spanish Central System. Geochimica et Cosmochimica Acta 69 (Supp. 1), A855.
Orejana, D., Villaseca, C., Paterson, B.A., 2006. Geochemistry of pyroxenitic and hornblenditic xenoliths in alkaline lamprophyres from the Spanish Central System. Lithos 86, 167–196.
Orejana, D., Villaseca, C., Billström, K., Paterson, B.A., 2008. Petrogenesis of Permian alkaline lamprophyres and diabases from the Spanish Central System and their geodynamic context within western Europe. Contributions to Mineralogy and Petrology 156, 457–500.
Peccerillo, A., Taylor, S.R., 1976. Geochemistry of Eocene calc–alkaline volcanic rocks from the Kastamonu area, northern Turkey. Contributions to Mineralogy and Petrology 58, 63–81.
Perini, G., Cebriá, J.M., López-Ruiz, J.M., Doblas, M., 2004. Carboniferous-Permian mafic magmatism in the Variscan Belt of Spain and France: implications for mantle sources. In: Wilson, M., Neumann, E.R., Davies, G.R., Timmerman, M.J., Heeremans, M., Larsen, B. (Eds.), Permo-Carboniferous Magmatism and Rifting in Europe. Geological Society of London Special Publication 223, London, pp. 415–438.
Philpotts, J.A., Schnetzler, C.C., 1970. Phenocryst-matrix partition coefficients for K, Rb, Sr and Ba, with applications to anorthosite and basalt genesis. Geochimica et Cosmochimica Acta 34, 307–322.
Pinarelli, L., Rottura, A., 1995. Sr and Nd isotopic study and Rb–Sr geochronology of the Béjar granites, Iberian Massif, Spain. European Journal of Mineralogy 7, 577–589.
Rehkamper, M., Hofmann, A.W., 1997. Recycled ocean crust and sediment in Indian Ocean MORB. Earth and Planetary Science Letters 147, 93–106.
Reyes, J., Villaseca, C., Barbero, L., Quejido, A.J., Santos, J.F., 1997. Descripción de un método de separación de Rb, Sr, Sm y Nd en rocas silicatadas para estudios isotópicos. Congreso Ibérico de Geoquímica I, 46–55.
Rudnick, R.L., Fountain, D.M., 1995. Nature and composition of the continental crust: a lower crustal perspective. Reviews of Geophysics 33, 267–309.
Rudnick, R.L., Gao, S., 2003. Composition of the continental crust. In: Holland, H.D., Turekian, K.K. (Eds.), Treatise on Geochemistry 3. The Crust. Elsevier-Pergamon, Oxford, pp. 1–64.
Rudnick, R.L., Goldstein, S.L., 1990. The Pb isotopic compositions of lower crustal xenoliths and the evolution of lower crustal Pb. Earth and Planetary Science Letters 98, 192–207.
Scarrow, J.H., Bea, F., Montero, P., Molina, J.F., Vaughan, A.P.M., 2006. A precise late Permian $^{40}Ar/^{39}Ar$ age for Central Iberian camptonitic lamprophyres. Geologica Acta 4, 451–459.
Shaw, D.M., 1970. Trace element fractionation during anatexis. Geochimica et Cosmochimica Acta 34, 237–243.
Simancas, J.F., Martínez Poyatos, D., Expósito, I., Azor, A., González Lodeiro, F., 2001. The structure of a major suture zone in the SW Iberian Massif: the Ossa–Morena/Central Iberian contact. Tectonophysics 332, 295–308.
Sun, S.S., McDonough, W.F., 1989. Chemical and isotopic systematics of oceanic basalts; implications for mantle composition and processes. Geological Society of London Special Publication 42, 313–345.
Turpin, L., Velde, D., Pinte, G., 1988. Geochemical comparison between minettes and kersantites from the western European Hercynian orogen: trace element and Pb–Sr–Nd isotope constraints on their origin. Earth and Planetary Science Letters 87, 73–86.
Ugidos, J.M., Recio, C., 1993. Origin of cordierite-bearing granites by assimilation in the Central Iberian Zone, Spain. Chemical Geology 103, 27–43.
Villaseca, C., Herreros, V., 2000. A sustained felsic magmatic system: the Hercynian granitic batholith of the Spanish Central System. Transactions of the Royal Society of Edinburgh: Earth Sciences 91, 207–219.
Villaseca, C., Barbero, L., Rogers, G., 1998. Crustal origin of Hercynian peraluminous granitic batholiths of central Spain: petrological, geochemical and isotopic (Sr,Nd) arguments. Lithos 43, 55–79.
Villaseca, C., Downes, H., Pin, C., Barbero, L., 1999. Nature and composition of the lower continental crust in central Spain and the granulite–granite linkage: inferences from granulitic xenoliths. Journal of Petrology 40, 1465–1496.
Villaseca, C., Orejana, D., Pin, C., López García, J.A., Andonaegui, P., 2004. Le magmatisme basique hercynien et post-hercynien du Système Central Espagnol: essai de caractèrisation des sources mantelliques. Comptes Rendus Géosciences 336, 877–888.
Villaseca, C., Orejana, D., Paterson, B., Billström, K., Pérez-Soba, C., 2007. Metaluminous pyroxene-bearing granulite xenoliths from the lower continental crust in central Spain: their role in the genesis of Hercynian I-type granites. European Journal of Mineralogy 19, 463–477.
Vilá, M., Pin, C., Enrique, P., Liesa, M., 2005. Telescoping of three distinct magmatic suites in an orogenic setting: generation of Hercynian igneous rocks of the Albera Massif (Eastern Pyrenees). Lithos 83, 97–127.
Wilson, M., 1989. Igneous petrogenesis. A Global Tectonic Approach. Unwin Hyman, Boston, p. 466.
Wilson, M., Downes, H., 1991. Tertiary-quaternary extension-related alkaline magmatism in western and central Europe. Journal of Petrology 32, 811–849.
Witt-Eickschen, G., Kramm, U., 1998. Evidence for the multiple stage evolution of the subcontinental lithospheric mantle beneath the Eifel (Germany) from pyroxenite and composite pyroxenite/peridotite xenoliths. Contributions to Mineralogy and Petrology 131, 258–272.
Witt-Eickschen, G., Seck, H.A., Mezger, K., Eggins, S.M., Altherr, R., 2003. Lithospheric mantle evolution beneath the Eifel (Germany): constraints from Sr–Nd–Pb isotopes and trace element abundances in spinel peridotite and pyroxenite xenoliths. Journal of Petrology 44, 1077–1095.
Zeck, H.P., Wingate, M.T.D., Pooley, G., 2007. Ion microprobe U–Pb zircon geochronology of a late tectonic granitic–gabbroic rock complex within the Iberian Hercynian Belt. Geological Magazine 144, 157–177.
Zindler, A., Hart, S.R., 1986. Chemical geodynamics. Annual Review of Earth and Planetary Sciences 14, 493–571.